primary tumor site could spread into the regional draining lymphatics, selectively replicate in neoplastic foci, and then reduce the number of tumor cells in metastatic lymph nodes in an orthotopic human colorectal cancer xenograft model. This virus-mediated molecular surgery for lymph node metastasis mimics the clinical scenario of lymphadenectomy; the technique, however, seems to be safer and less invasive. Moreover, we demonstrated that preoperative delivery of OBP-301 into primary tumors prevented the exacerbation of lymph node metastasis by surgical procedures. OBP-301 may offer advantages over other oncolytic viruses targeting lymphatic metastasis, as its safety profile as well as biodistribution pattern after intratumoral delivery have already been confirmed in a phase I clinical trial for various types of solid tumors.[14] The current study provides evidence for the in vivo purging effect of OBP-301 in regional lymph nodes that is sufficiently reliable to support this approach. Thus, phase II studies of telomerase-specific virotherapy targeting lymph node metastasis in human cancer patients are warranted.

ACKNOWLEDGMENTS

The authors thank Daiju Ichimaru (Oncolys BioPharma, Inc.) for the helpful discussion. The authors also thank Tomoko Sueishi and MitsukoYokota for the excellent technical support.

REFERENCES

1. Maehara Y, Oshiro T, Endo K, et al. Clinical significance of occult micrometastasis lymph nodes from patients with early gastric cancer who died of recurrence. *Surgery*. 1996;119:397–402.
2. Rivadeneira DE, Simmons RM, Christos PJ, et al. Predictive factors associated with axillary lymph node metastases in T1a and T1b breast carcinomas: analysis in more than 900 patients. *J Am Coll Surg*. 2000;191:1–6.
3. Chang GJ, Rodriguez-Bigas MA, Skibber JM, et al. Lymph node evaluation and survival after curative resection of colon cancer: systematic review. *J Natl Cancer Inst*. 2007;99:433–441.
4. Volpe CM, Koo J, Miloro SM, et al. The effect of extended lymphadenectomy on survival in patients with gastric adenocarcinoma. *J Am Coll Surg*. 1995;181:56–64.
5. Harrison LE, Karpeh MS, Brennan MF. Extended lymphadenectomy is associated with a survival benefit for node-negative gastric cancer. *J Gastrointest Surg*. 1998;2:126–131.
6. Sasako M, Sano T, Yamamoto S, et al. D2 lymphadenectomy alone or with para-aortic nodal dissection for gastric cancer. *N Engl J Med*. 2008;359:453–462.
7. Gotoda T, Sasako M, Ono H, et al. Evaluation of the necessity for gastrectomy with lymph node dissection for patients with submucosal invasive gastric cancer. *Br J Surg*. 2001;88:444–449.
8. Liu TC, Galanis E, Kirn D. Clinical trial results with oncolytic virotherapy: a century of promise, a decade of progress. *Nat Clin Pract Oncol*. 2007;4:101–117.
9. Kirn DH, Thorne SH. Targeted and armed oncolytic poxviruses: a novel multi-mechanistic therapeutic class for cancer. *Nat Rev Cancer*. 2009;9:64–71.
10. Fujiwara T. Telomerase-specific virotherapy for human squamous cell carcinoma. *Expert Opin Biol Ther*. 2009;9:321–329.
11. Kawashima T, Kagawa S, Kobayashi N, et al. Telomerase-specific replication-selective virotherapy for human cancer. *Clin Cancer Res*. 2004;10:285–292.
12. Umeoka T, Kawashima T, Kagawa S, et al. Visualization of intrathoracically disseminated solid tumors in mice with optical imaging by telomerase-specific amplification of a transferred green fluorescent protein gene. *Cancer Res*. 2004;64:6259–6265.
13. Taki M, Kagawa S, Nishizaki M, et al. Enhanced oncolysis by a tropism-modified telomerase-specific replication-selective adenoviral agent OBP-405 (Telomelysin-RGD). *Oncogene*. 2005;24:3130–3140.
14. Fujiwara T, Tanaka N, Numunaitis JJ, et al. Phase I trial of intratumoral administration of OBP-301, a novel telomerase-specific oncolytic virus, in patients with advanced solid cancer: evaluation of biodistribution and immune response. *J Clin Oncol*. 2008;26:3572.
15. Kishimoto H, Kojima T, Watanabe Y, et al. In vivo imaging of lymph node metastasis with telomerase-specific replication-selective adenovirus. *Nat Med*. 2006;12:1213–1219.
16. Johnson M, Huyn S, Burton J, et al. Differential biodistribution of adenoviral vector in vivo as monitored by bioluminescence imaging and quantitative polymerase chain reaction. *Hum Gene Ther*. 2006;17:1262–1269.
17. Burton JB, Johnson M, Sato M, et al. Adenovirus-mediated gene expression imaging to directly detect sentinel lymph node metastasis of prostate cancer. *Nat Med*. 2008;14:882–888.
18. Schneider T, Osl F, Friess T, et al. Quantification of human Alu sequences by real-time PCR—an improved method to measure therapeutic efficacy of anti-metastatic drugs in human xenotransplants. *Clin Exp Metastasis*. 2002;19:571–582.
19. Zijlstra A, Mellor R, Panzarella G, et al. A quantitative analysis of rate-limiting steps in the metastatic cascade using human-specific real-time polymerase chain reaction. *Cancer Res*. 2002;62:7083–7092.
20. Umetani N, Giuliano AE, Hiramatsu SH, et al. Prediction of breast tumor progression by integrity of free circulating DNA in serum. *J Clin Oncol*. 2006;24:4270–4276.
21. Kariya Y, Kato K, Hayashizaki Y, et al. Revision of consensus sequence of human Alu repeats—a review. *Gene*. 1987;53:1–10.
22. Liu TC, Kirn D. Systemic efficacy with oncolytic virus therapeutics: clinical proof-of-concept and future directions. *Cancer Res*. 2007;67:429–432.
23. Kurihara Y, Watanabe Y, Onimatsu H, et al. Telomerase-specific virotheranostics for human head and neck cancer. *Clin Cancer Res*. 2009;15:2335–2343.
24. Kawabata K, Sakurai F, Koizumi N, et al. Adenovirus vector-mediated gene transfer into stem cells. *Mol Pharm*. 2006;3:95–103.
25. Hiyama K, Hirai Y, Kyoizumi S, et al. Activation of telomerase in human lymphocytes and hematopoietic progenitor cells. *J Immunol*. 1995;155:3711–3715.
26. Burdelya LG, Krivokrysenko VI, Tallant TC, et al. An agonist of toll-like receptor 5 has radioprotective activity in mouse and primate models. *Science*. 2008;320:226–230.
27. Folkman J. Role of angiogenesis in tumor growth and metastasis. *Semin Oncol*. 2002;29:15–18.

© 2010 Lippincott Williams & Wilkins

Research Article

Molecular Cancer Therapeutics

Preclinical Evaluation of Differentially Targeting Dual Virotherapy for Human Solid Cancer

Ryo Sakai[1], Shunsuke Kagawa[1,2], Yasumoto Yamasaki[1], Toru Kojima[1], Futoshi Uno[1,2], Yuuri Hashimoto[1,3], Yuichi Watanabe[1,3], Yasuo Urata[3], Noriaki Tanaka[1], and Toshiyoshi Fujiwara[1,2]

Abstract

Multimodal approaches combining drugs that differentially function is the most popular regimen for treating human cancer. Understanding the molecular mechanisms underlying the synergistic, potentiative, and antagonistic effects of drug combinations could facilitate the discovery of novel efficacious combinations. We previously showed that telomerase-specific replication-competent adenovirus (Telomelysin, OBP-301), in which the human telomerase reverse transcriptase promoter controls the adenoviral E1 gene expression, induces a selective antitumor effect in human cancer cells. Here, using E1-deleted replication-deficient adenovirus expressing the p53 tumor suppressor gene (Advexin, Ad-p53) and OBP-301, we investigate how these adenoviruses that kill tumor cells with different mechanisms could work in combination on human cancer. We found that E1-deficient Ad-p53 could kill cancer cells more efficiently in the presence of OBP-301 than Ad-p53 alone or OBP-301 alone, because Ad-p53 could become replication-competent by being supplied adenoviral E1 from coinfected OBP-301 in trans. Ad-p53 plus OBP-301 induced high levels of p53 protein expression without p21 induction, resulting in apoptotic cell death documented by active caspase-3 expression with a cytometric bead array and an increased subdiploid apoptotic fraction of the cell cycle. For *in vivo* evaluation, nude mice xenografted with human lung tumors received intratumoral injection of OBP-301 and/or Ad-p53. Analysis of the growth of implanted tumors showed an enhanced antitumor effect in combination therapy. Our data show that Ad-p53 in combination with OBP-301 induces not only oncolytic but also apoptotic cancer cell death and enhances antitumor activity *in vitro* and *in vivo*, providing potential merits as a multimodal treatment for human cancer. *Mol Cancer Ther; 9(6); 1884–93. ©2010 AACR.*

Introduction

Combining antineoplastic agents with different mechanisms of action has resulted in many effective regimens in cancer therapy. For example, biochemical modulation of 5-fluorouracil, one of the most active single agents presently available, with the reduced folate leucovorin has significantly improved overall response rates in the 25% to 30% range (1). To successfully achieve synergistic effects, we need to elucidate the biochemical and/or molecular mechanisms underlying the drug interaction. Recent advances in understanding the molecular mechanisms of carcinogenesis allow us to develop a number of molecularly targeted therapies. Most agents have been developed to target specific molecules which are essential for the acquisition of malignant phenotypes such as proliferation, invasion, and metastasis.

Gene- and vector-based therapies, which have long been viewed as unsuccessful, have been greatly rejuvenated by its combination with other modalities including chemotherapy and radiotherapy (2, 3). It also remains possible to increase the therapeutic benefit by combining virotherapies having different targets. Ad-p53 (Advexin, Ad5CMV-p53) consists of an E1-deleted replication-deficient type 5 adenoviral vector expressing the human wild-type p53 tumor suppressor gene under the control of a cytomegalovirus promoter. p53 is the most commonly mutated gene in human cancer (4, 5), and p53 gene therapy using Ad-p53 is currently in clinical trials as a cancer therapy (6–9); however, a number of limitations have led to the suboptimal efficacy of existing gene therapies. One reason is that replication-deficient adenoviruses infect only a small portion of the tumor and are not able to spread over the tumor entirely. To improve viral spread in tumor conferring specificity of infection, replication-competent adenoviruses have been investigated (10–12).

Authors' Affiliations: [1]Department of Gastroenterological Surgery, Okayama University Graduate School of Medicine, Dentistry, and Pharmaceutical Sciences, [2]Center for Gene and Cell Therapy, Okayama University Hospital, Okayama, Japan; and [3]Oncolys BioPharma, Inc., Tokyo, Japan

Corresponding Author: Toshiyoshi Fujiwara, Department of Gastroenterological Surgery, Okayama University Graduate School of Medicine, Dentistry, and Pharmaceutical Sciences, 2-5-1 Shikata-cho, Kita-ku, Okayama 700-8558, Japan. Phone: 81-86-235-7257; Fax: 81-86-221-8775. E-mail: toshi_f@md.okayama-u.ac.jp

doi: 10.1158/1535-7163.MCT-10-0205

©2010 American Association for Cancer Research.

We previously developed a telomerase-specific, replication-competent adenovirus (Telomelysin, OBP-301), in which the human telomerase reverse transcriptase (hTERT) promoter element drives the adenoviral E1 gene, and induced a selective antitumor effect in human cancer cells (13–17). Telomerase is a ribonucleoprotein complex responsible for the complete replication of chromosomal ends (18). Many studies have shown the expression of telomerase activity in more than 85% of human cancers (19), but only in few normal somatic cells (20). Telomerase activation is considered a critical step in carcinogenesis and its activity is closely correlated with hTERT expression (21). Although virotherapy using OBP-301 as a monotherapy is currently being evaluated in clinical trials (22), multimodal strategies to enhance antitumor efficacy *in vivo* might be essential for a successful clinical outcome.

As a replication-deficient adenovirus could replicate in cancer cells and enhance the anticancer effect when co-transfected with a replication-competent adenovirus that could produce E1 proteins, we reasoned that combined treatment with Ad-p53 and OBP-301 might offer a way to more efficiently kill human tumor cells. In the present study, we investigated the synergistic effects of Ad-p53 combined with OBP-301 both *in vitro* and *in vivo*.

Materials and Methods

Cell lines and cell cultures

The human non–small cell lung cancer cell line H1299, which has a homozygously deleted p53, and the human colorectal carcinoma cell line SW620, which contains mutated p53, were propagated in monolayer culture in RPMI 1640 supplemented with 10% FCS, 100 units/mL of penicillin, and 100 μg/mL of streptomycin.

Recombinant adenoviruses

The recombinant replication-selective, tumor-specific adenovirus vector OBP-301 (Telomelysin), in which the hTERT promoter element drives the expression of E1A and E1B genes linked with an IRES, was constructed and characterized previously (16). Replication-deficient adenoviral vectors containing human wild-type p53 cDNA (Ad-p53) and β-galactosidase cDNA (Ad-lacZ) were also used (23). These viruses were purified by $CsCl_2$ step gradient ultracentrifugation followed by $CsCl_2$ linear

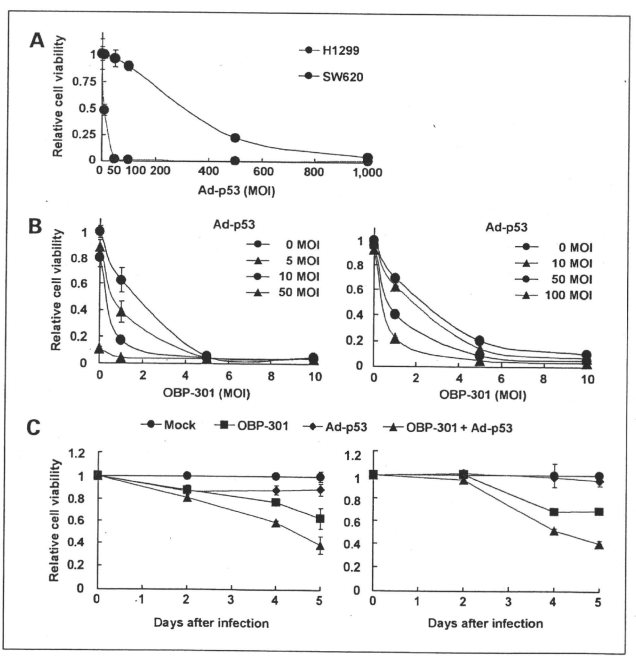

Figure 1. A, effect of Ad-p53 on human cancer cell lines. H1299 and SW620 cells were infected with 0, 10, 50, 100, 500, and 1,000 MOIs of Ad-p53. Cell viability was assessed by XTT assay 5 d after infection. B, dose-response analysis of cell viability in combination therapy. H1299 (left) and SW620 (right) cells were treated with the indicated MOIs of Ad-p53, OBP-301, or a combination of both simultaneously. The cell-killing effect was evaluated by XTT assay 5 d after infection. C, time course analysis of cell viability in combination therapy. H1299 (left) and SW620 (right) cells were treated with 1 MOI of OBP-301, 5 MOI (for H1299) or 50 MOI (for SW620) of Ad-p53, or a combination of both at the same time. Cell viability was assessed by XTT assay 2, 4, and 5 d after infection. Bars, SD.

gradient ultracentrifugation, and their titers were determined by plaque assay in the 293 cells.

Cell proliferation assay

Cells were seeded at 1,000 cells/well in 96-well plate and infected with OBP-301, Ad-p53, or OBP-301 and Ad-p53 simultaneously at the indicated multiplicities of infection (MOI) 18 to 20 hours later. Cell viability was assessed at the indicated times after adenoviral infection using sodium 3′-[1-(phenylaminocarbonyl)-3,4-tetrazolium]-bis(4-methoxy-6-nitro) benzene sulfonic acid hydrate (XTT) assay with the Cell Proliferation Kit II (Roche Molecular Biochemicals) according to the protocol provided by the manufacturer.

Western blot analysis

The primary antibodies against p53 (Ab-2; Calbiochem), p21 (EA10; Oncogene Science), β-actin (AC-15; Sigma Chemical, Co.), and peroxidase-linked secondary antibody (Amersham) were used. Cells were washed twice in cold PBS and collected then lysed in lysis buffer [10 mmol/L Tris (pH 7.5), 150 mmol/L NaCl, 50 mmol/L NaF, 1 mmol/L EDTA, 10% glycerol, and 0.5% NP40] containing proteinase inhibitors (0.1 mmol/L phenylmethylsulfonyl fluoride and 0.5 mmol/L Na_3VO_4). After 20 minutes on ice, the lysates were spun at 14,000 rpm in a microcentrifuge at 4°C for 5 minutes. The supernatants were used as whole cell extracts. Protein concentration was determined using the Bio-Rad protein determination method (Bio-Rad). Equal amounts of proteins were boiled for 5 minutes and electrophoresed under reducing conditions in 4% to 12% (w/v) polyacrylamide gels. Proteins were electrophoretically transferred to Hybond polyvinylidene difluoride transfer membranes (Amersham Life Science) and incubated with the primary antibody followed by peroxidase-linked secondary antibody. An Amersham ECL chemiluminescent western system (Amersham) was used to detect secondary probes.

Human apoptosis cytometric bead array for active caspase-3

Caspase-3 activation was quantitated using the Human Apoptosis Cytometric Bead Array kit (Becton Dickinson) according to the instructions of the manufacturer. Briefly, cell lysates were incubated with cytometric caspase-3 capture beads coated with antibody specific for caspase-3 and a secondary antibody specific for the cleaved site of active caspase-3 conjugated to phycoerythrin. Cytometric bead/caspase-3 conjugates were analyzed by flow cytometry using a FACSCalibur (Becton Dickinson). Flow cytometry measures the amount of active caspase-3 attached to beads. Becton Dickinson Cytometric Bead Array software was used to analyze beads and transform data from samples. Sample data

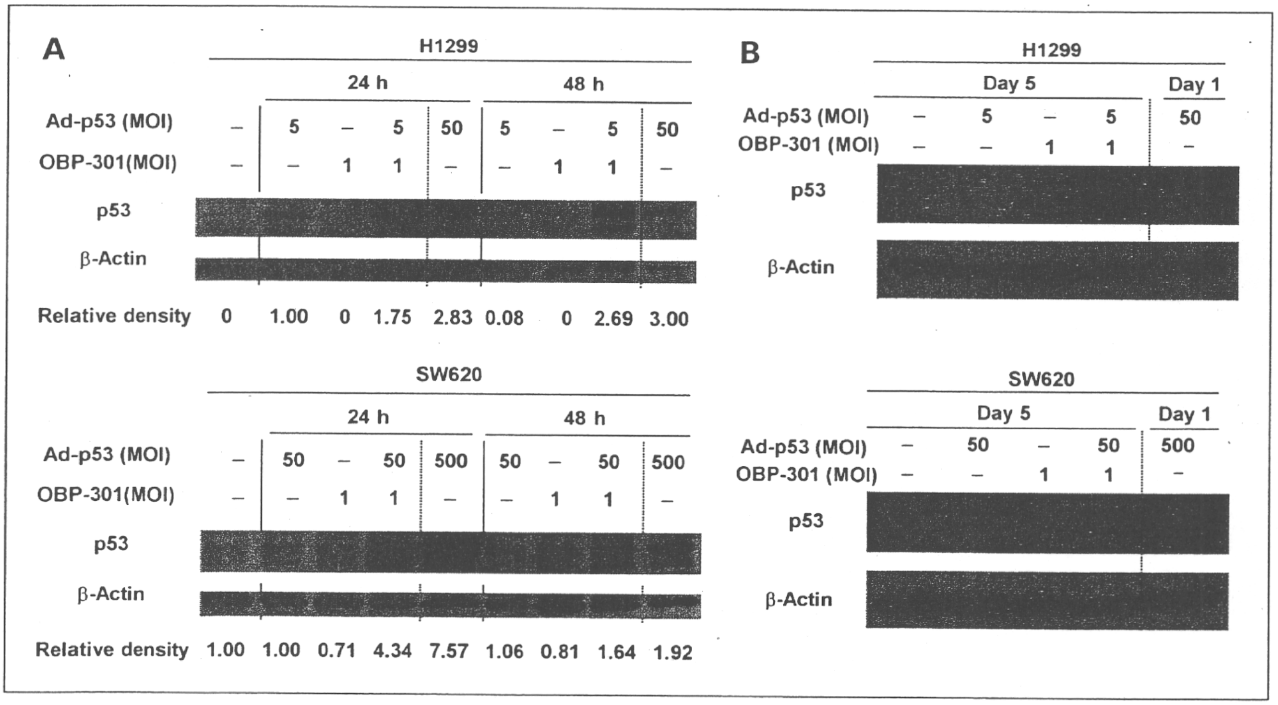

Figure 2. Expression of p53 in combination therapy of Ad-p53 and OBP-301. H1299 and SW620 cells were infected with the indicated viruses and harvested at the indicated time. Cell lysates were subjected to immunoblot analysis for p53 and β-actin. H1299 cells infected with 50 MOI of Ad-p53 and SW620 cells infected with 500 MOI of Ad-p53 were used as a positive control for apoptosis. A, cells were harvested in the early phase (24 and 48 h after infection). p53 expression level was quantified by densitometric scanning using NIH Image software and normalization by dividing the β-actin signal. The background was subtracted and corrected so that the control became 0, because H1299 cells were p53-null. B, cells were harvested in the late phase (5 d after infection).

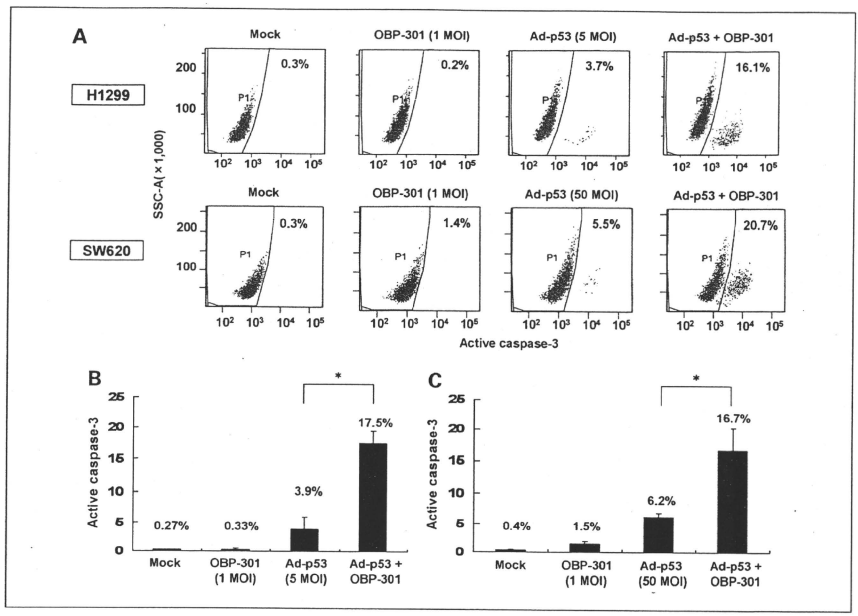

Figure 3. Induction of apoptosis in H1299 and SW620 cells following infection with Ad-p53 plus OBP-301. H1299 and SW620 cells were infected with the indicated MOIs of OBP-301, Ad-p53, or a combination of both simultaneously. Caspase-3 activation was quantitated using the cytometric bead array (CBA) assay 48 h after infection. A, representative flow cytometric images are shown. B and C, active caspase-3 expression was significantly increased after infection with Ad-p53 plus OBP-301 in H1299 (B) and SW620 (C) cells. Columns, mean of three experiments; bars, SE. *, $P < 0.01$, statistical significance (Student's t test).

was normalized with specific protein standards to provide quantification of the proteins of interest.

In vitro replication assay

H1299 cells were infected with OBP-301 (1 MOI), Ad-p53 (5 MOI), OBP-301 (1 MOI) + Ad-p53 (5 MOI), or OBP-301 (1 MOI) + Ad-lacZ (5 MOI) for 24 hours after seeding for 2 hours. Following the removal of virus inocula, the cells were further incubated at 37°C, trypsinized, and harvested at 2, 24, 48, and 72 hours after infection. DNA purification was done using QIAmp DNA mini kit (Qiagen, Inc.). The E1A and p53 DNA copy numbers were determined by quantitative real-time PCR using a LightCycler instrument and LightCycler-DNA Master SYBR Green I (Roche Diagnostics).

Cell cycle analysis

Cells treated with various concentrations of OBP-301, Ad-p53, or a combination of both were harvested in 0.125% trypsin, washed twice in PBS with 2% FCS. After centrifugation, 1×10^6 cells were resuspended in 70% ethanol at 4°C overnight. Cells were washed twice in PBS. After centrifugation, the pellet was resuspended in 0.25 μg/mL of RNase A for 30 minutes at 37°C. The samples were then stained with 50 μg/mL of propidium iodide and incubated at 4°C for 30 minutes. Cell cycle analysis was determined by FACSCalibur flow cytometer using FlowJo software (TreeStar, Inc.).

In vivo human tumor model

H1299 cells (7.5×10^6 cells/mouse) were injected s.c. into the flank of 5-week-old female BALB/c *nu/nu* mice and permitted to grow to 4 to 10 mm in diameter. At that time, the mice were randomly assigned into six groups, and a 50 μL solution containing Ad-p53 [1×10^9 plaque-forming units (pfu)], OBP-301(1×10^7 pfu), OBP-301 (1×10^7 pfu) + Ad-p53 (1×10^8 pfu), or Ad-lacZ (1×10^8 pfu), Ad-p53 (1×10^8 pfu) + Ad-lacZ (1×10^7 pfu), or PBS was injected into the tumor for three cycles every 2 days. The perpendicular diameter of each tumor was measured every 3 or 4 days, and tumor volume was calculated using the following formula:

tumor volume (mm^3) = $a \times b^2 \times 0.5$, where a is the longest diameter, b is the shortest diameter and 0.5 is a constant to calculate the volume of an ellipsoid. The experimental protocol was approved by the Ethics Review Committee for Animal Experimentation of Okayama University School of Medicine.

Statistical analysis

The statistical significance of the differences in the *in vitro* and *in vivo* antitumor effects of viruses was determined by using the (two-tailed) Student's *t* test.

Results

Enhanced antitumor effect of OBP-301 plus Ad-p53 in human cancer cell lines *in vitro*

To achieve optimum antitumor effect, Ad-p53 at the MOI of 50 and 500 was needed in H1299 and SW620 cells, respectively (Fig. 1A). We have previously confirmed that these cells expressed detectable hTERT mRNA (13, 14). To examine the potential interaction of Ad-p53 with OBP-301, we did a dose-response analysis of the cell-killing effect at various doses in H1299 and SW620 cells. Ad-p53 at 5 or 50 MOI could have little antitumor effect in H1299 and SW620 cells, respectively. Combination therapy with 1 MOI of OBP-301 plus Ad-p53 resulted in more cell killing than OBP-301 alone or Ad-p53 alone in both cells (Fig. 1B). In contrast, OBP-301 plus Ad-lacZ did not increase the antitumor effect (data not shown). We next examined a time course analysis of the cell-killing effect. The antitumor effect of Ad-p53 plus OBP-301 was augmented after 4 days of infection (Fig. 1C). To determine whether the timing of administration of the adenoviruses affected the combined cytotoxic effect, H1299 and SW620 cells were treated with Ad-p53 24 hours after infection or synchronously with OBP-301. The results showed no apparent differences in cytotoxic activity by the treatment schedules (data not shown).

Increased expression of p53 by cotransduction with OBP-301 and Ad-p53

To explore the effect of the combination of Ad-p53 and OBP-301, the expression levels of p53 protein were compared by immunoblotting analyses at 24 and 48 hours after infection. By cotransduction with Ad-p53 and OBP-301, the expression of p53 was 33.6-fold higher in H1299 cells at 48 hours and 4.34-fold higher in SW620

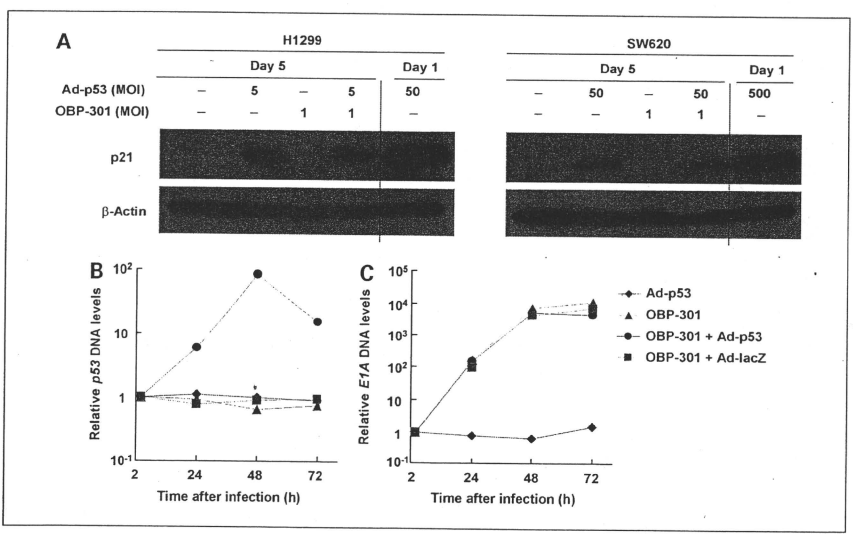

Figure 4. A, expression of p53 downstream mediator p21. H1299 and SW620 cells were infected with the indicated viruses and harvested at the indicated times. Cell lysates were subjected to immunoblot analyses for p21 and β-actin. H1299 cells infected with 50 MOI of Ad-p53 and SW620 cells infected with 500 MOI of Ad-p53 were used as a positive control for p21 induction. B and C, assessment of viral DNA replication in H1299 cells. H1299 cells were infected with OBP-301 (1 MOI), Ad-p53 (5 MOI), OBP-301 (1 MOI) + Ad-p53 (5 MOI), or OBP-301 (1 MOI) + Ad-lacZ (5 MOI) for 2 h. Following the removal of virus inocula, the cells were further incubated at 37°C, trypsinized, and harvested at 2, 24, 48, and 72 h after infection. Extracted DNA was subjected to real-time PCR assay for p53 DNA (B) and E1A DNA (C).

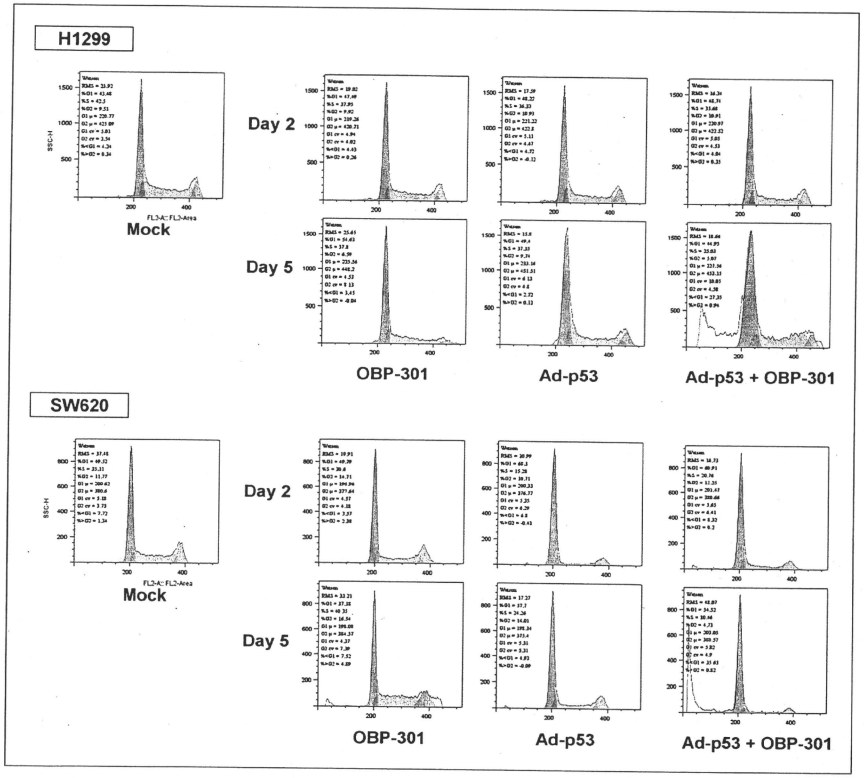

Figure 5. H1299 cells were infected with 1 MOI of OBP-301, 5 MOI of Ad-p53, or a combination of both and harvested on days 2 and 5. SW620 cells were infected with 1 MOI of OBP-301, 50 MOI of Ad-p53, or a combination of both and harvested on days 2 and 5. Cells were stained with propidium iodide. Then, cell cycle analysis was determined by the fluorescence-activated cell sorter (FACSCalibur) flow cytometer.

cells at 24 hours than by Ad-p53 alone (Fig. 2A). The augmented expression of p53 was maintained in cotransduced cells with both adenoviruses on day 5 (Fig. 2B). The prolonged upregulation of p53 suggests that Ad-p53 replicates in cancer cells by E1 protein supplied by cotransduced OBP-301, although the pattern of increased p53 expression was different between H1299 and SW620 cells. These cells expressed equivalent levels of coxsackievirus and adenovirus receptor (15); p53-null H1299 cells were, however, more sensitive to Ad-p53 compared with SW620 cells containing mutated p53, as shown in Fig. 1A, suggesting that Ad-p53 induced rapid apoptosis within 48 hours in infected H1299 cells and, therefore, p53 expression declined at 48 hours after infection. In contrast, as Ad-p53 could replicate and infect more H1299 cells in the presence of OBP-301, the level of p53 expression increased after coinfection of Ad-p53 and OBP-301.

Combined treatment of OBP-301 plus Ad-p53 more efficiently induced apoptosis

Overexpression of p53 is known to induce apoptosis in most cancer cells. We hypothesized that the enhanced antitumor effect of Ad-p53 plus OBP-301 would result in elevated apoptotic cell death. Two days after infection, combined treatment of Ad-p53 plus OBP-301 induced significantly elevated levels of active caspase-3, whereas a low dose of Ad-p53 alone did not (Fig. 3). Moreover, interestingly, the expression level of p21, which is a

downstream target of p53 in combination therapy with OBP-301 and Ad-p53, was lower than in low doses of Ad-p53 alone (Fig. 4A).

p53 DNA copy number is significantly amplified in combination therapy with OBP-301 and Ad-p53, whereas p53 does not impair the replication of OBP-301

Then we examined the p53 DNA levels in H1299 cells. The amplification of p53 DNA in the cells treated with Ad-p53 plus OBP-301 by one to two orders of magnitude was observed (Fig. 4B). These results suggest that Ad-p53 actually replicates by using the E1 protein supplied by OBP-301, which is consistent with increased expression of p53 protein (Fig. 2A). In this combination treatment, proapoptotic p53 expression might impair the replication of oncolytic virus because of premature early cell death provoked by p53. Therefore, we examined the effect of p53 on the replication of OBP-301 by quantitative real-time PCR analysis. H1299 cells were infected with OBP-301 and/or Ad-p53. Cells were harvested 2, 24, and 48 hours after infection, and extracted DNA were subjected to the assay. As shown in Fig. 4C, the presence of Ad-p53 did not impair the replication of OBP-301.

Augmentation of apoptosis in human tumor cells after coinfection with Ad-p53 and OBP-301

We next did a cell cycle analysis in H1299 and SW620 cells on days 2 and 5 after infection. Neither group showed any differences between treatment 2 days after infection; however, a sub-G_1 population (an apoptotic cell population) was markedly increased in H1299 and SW620 cells infected with Ad-p53 plus OBP-301 after 5 days of infection, whereas OBP-301 or Ad-p53 alone did not increase apoptosis (Fig. 5; Table 1). These results were compatible with those of the time course analyses (Fig. 1C), suggesting that the augmented antitumor effect of combined treatment of Ad-p53 and OBP-301 was due to enhanced apoptotic cancer cell death.

Antitumor effect of OBP-301 plus Ad-p53 in human tumor xenografts

Based on the *in vitro* combination effect of Ad-p53 and OBP-301, the *in vivo* therapeutic efficacy of H1299 tumors was further assessed. Mice bearing H1299-xenografted tumors measuring 4 to 10 mm in diameter received intratumoral injection of Ad-p53 at a dose of 1×10^8 pfu and OBP-301 at a dose of 1×10^7 pfu, singly or in combination every 2 days for three cycles starting at day 0. As shown in Fig. 6, Ad-p53 alone and Ad-p53 + Ad-lacZ had no apparent antitumor effect, but OBP-301 alone resulted in significant tumor suppression compared with controls ($P < 0.05$). OBP-301 plus Ad-lacZ did not improve the tumor suppression compared with OBP-301 alone ($P > 0.05$). Nevertheless, the combination of OBP-301 plus Ad-p53 produced a more profound and significant inhibition of tumor growth compared with OBP-301 alone or OBP-301 plus Ad-lacZ ($P < 0.05$).

Table 1. Cell cycle analysis following infection with OBP-301, Ad-p53, or Ad-p53 plus OBP-301 in H1299 and SW620 cells

Cell lines	Days	Treatments	Cell cycle distribution (%)			
			Sub–G_0-G_1	G_0-G_1	S	G_2-M
H1299		Mock	4.51	43.48	42.5	9.51
	Day 2	OBP-301	4.64	47.49	37.95	9.92
		Ad-p53	4.52	48.22	36.33	10.93
		Ad-p53 + OBP-301	4.67	48.74	35.68	10.91
	Day 5	OBP-301	0.98	54.63	37.8	6.59
		Ad-p53	3.51	49.4	37.35	9.74
		Ad-p53 + OBP-301	24.95	44.95	25.03	5.07
SW620		Mock	3.06	49.52	35.11	11.77
	Day 2	OBP-301	4.9	49.79	30.6	14.71
		Ad-p53	5.71	68.3	15.28	10.71
		Ad-p53 + OBP-301	7.08	60.91	20.76	11.25
	Day 5	OBP-301	5.93	37.18	40.35	16.54
		Ad-p53	4.03	57.7	24.26	14.01
		Ad-p53 + OBP-301	30.29	54.52	10.46	4.73

NOTE: H1299 cells were infected with 1 MOI of OBP-301, 5 MOI of Ad-p53, or a combination of both and harvested on days 2 and 5. SW620 cells were infected with 1 MOI of OBP-301, 50 MOI of Ad-p53, or a combination of both and harvested on days 2 and 5. Cell cycle analysis was determined by the fluorescence-activated cell sorter (FACSCalibur) flow cytometer.

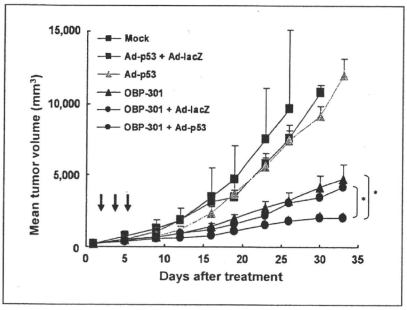

Figure 6. H1299 cells (7.5×10^6 cells/mouse) were injected s.c. into the flank of BALB/c *nu/nu* mice and permitted to grow to 4 to 10 mm in diameter. A 50 μL solution containing Ad-p53 (1×10^9 pfu), OBP-301 (1×10^7 pfu), OBP-301 (1×10^7 pfu) + Ad-p53 (1×10^8 pfu), or Ad-lacZ (1×10^8 pfu), Ad-p53 (1×10^8 pfu) + Ad-lacZ (1×10^7 pfu), or PBS was injected into the tumor for three cycles every 2 d. The perpendicular diameter of each tumor was measured every 3 or 4 d. Six or seven mice were used for each group. Points, mean tumor growth volume; bars, SE. *, $P < 0.05$, statistical significance (Student's *t* test). Arrows, days of treatment.

Discussion

Resistance to apoptosis is a major cause of treatment failure in human cancers. Many combination regimens with clinically available agents are currently being used; however, there is a need for a better understanding of the molecular interaction of drugs to efficiently induce apoptosis in human cancer cells. In the present study, our goal was to determine whether dual virotherapy, which mediates telomerase-specific enhancement of exogenous wild-type p53 gene expression, was effective for inducing apoptosis. We found that Ad-p53 and OBP-301, with different mechanisms of action, could be more effective in the growth of human cancer cells than Ad-p53 or OBP-301 alone *in vitro* as well as *in vivo*. Moreover, our data suggest that p53-induced p21 induction was inhibited in the presence of OBP-301 infection, which might in turn sensitize tumor cells to apoptosis by blocking cell cycle arrest.

Virotherapy for p53 gene transfer by Ad-p53 (Advexin) is currently in clinical trials as a cancer therapeutic (24). Overexpression of p53 gene caused preferential cancer cell–killing, although this was less toxic to normal cells, which means that p53 gene therapy itself is a cancer-targeting therapy; however, the low transduction rate and the narrow spread of Ad-p53 limits the anticancer effect *in vivo*. The major problem for p53 therapy with replication-defective adenovirus vector is incomplete transduction of target cancer cells. Therefore, cancer cells beyond transduced cells will escape the antitumor effect. To overcome the low transduction rate of replication-defective adenoviral vectors, an increment in the dose would be the simple resolution; however, a higher dose of Ad-p53 might not always contribute to the improvement of transduction efficacy and could potentially cause side effects. In this study, even the low dose of Ad-p53, administration of which solely was not enough to induce apoptosis, enabled an increase anticancer effect in combination with OBP-301 by replicating selectively in tumor cells. OBP-301 was genetically designed to replicate specifically in tumor cells, causing specific "oncolysis"(13, 15, 16), thereby increasing the effective treatment radius in tumors. This combination might contribute to the mitigation of unfavorable effects. OBP-301 is currently being evaluated in phase I trials for clinical safety as of the writing of this article.

Virotherapy with adenovirus Onyx-015, the first oncolytic virus, has been evaluated in clinical trials, and showed that administration of oncolytic adenovirus via intratumor, intraperitoneum, or intravenous methods was well tolerated (25); however, the efficacy of Onyx-015 as a single agent is also limited, possibly because of inefficient cell lysis and release of their progeny, which may be defective in cancer cells. Our strategy is aiming not only to enhance the antitumor activity of Ad-p53 by OBP-301, but also to augment the oncolytic activity of OBP-301 in combination with Ad-p53. Oncolysis is due to cytopathic effects intrinsic to the adenovirus. Adenovirus must be able to induce cell death in infected cells for the virus to generate a cytopathic effect and be released from the cell. Hall et al. showed that wild-type p53 enhances the ability of adenoviruses to induce cell death, whereas the loss of functional p53 in cancer cells resulted in a defect in adenovirus-induced cytopathic effects (26). Thus, functional p53 is required for a productive adenovirus infection. Consistent with their report, our strategy to compensate or overexpress functional wild-type p53 must be conducive to efficient adenovirus replication, which leads to effective oncolysis by OBP-301.

The efficacy of combination therapy with conventional gene therapy using replication-deficient adenovirus plus virotherapy has been reported previously (27, 28). Combined with tumor-specific replication-selective adenovirus, replication-deficient adenoviruses were able to replicate and spread to surrounding tumor cells. Antitumor activity was increased compared with gene therapy alone or virotherapy alone in agreement with our study. In our previous study, co-infection with a replication-deficient adenovirus expressing the green fluorescent protein (*GFP*) gene and OBP-301 was able to specifically visualize human lung cancer cells in an orthotopic murine model (14). Although the study showed the diagnostic application of combinative use of replication deficient adenoviral vector and OBP-301, the specific replication of coinfected adenovirus in tumor was visually evidenced. The current study applied this principle to therapeutic purpose. When Ad-p53 was used together with OBP-301, the total amount of the viruses might be higher than that of OBP-301 alone that shows the equivalent efficacy; the dose of replicative OBP-301, however, should be reduced as much as possible from the viewpoint of safety.

Indeed, the pharmacodynamic data in a phase I clinical trial of OBP-301 showed the transient systemic dissemination of OBP-301 following intratumoral injection (29).

Another interesting finding in the current study is that OBP-301 infection apparently inhibited exogenous p53-mediated expression of p21, which is a key player in arresting cells in the G_1 phase. This suggests that OBP-301 infection might be an important requirement for rendering tumor cells sensitive to apoptosis rather than cell cycle arrest. Indeed, it has been reported that the adenovirus E1A protein could enhance the sensitivity of tumor cells to chemotherapeutic agents by promoting apoptosis (30). This is primarily because of the ability of E1A to interact with p21 and thereby inactivate it, which in turn, leads to apoptosis. Further mechanisms of this interaction are now under investigation.

Our strategies aim to enhance the efficiency and specificity of viral agents through incorporation of tumor-targeting mechanisms via therapeutic gene and transcriptional regulation. Although this study examined the combinative use of two viral agents, oncolytic adenoviruses carrying therapeutic genes in the E1 or E3 region have also been reported (31, 32). Gene therapy and oncolytic virotherapy, however, do not always work effectively in combination (33). In case the expression level of therapeutic genes needs to be titrated, therapeutic genes might work better when separated from oncolytic virus. In addition, both p53 therapy and OBP-301 oncolytic therapy are currently being tested clinically. Once they are approved for clinical use, this study would provide realistic therapeutic applications as a preclinical study in the future.

In conclusion, our data showed that combination therapy of Ad-p53 and OBP-301 efficiently inhibited human cancer cell growth *in vitro* and *in vivo*, and that this approach has important implications for the treatment of human cancers.

Disclosure of Potential Conflicts of Interest

Y. Urata: employee of Oncolys BioPharma, Inc. T. Fujiwara: consultant to Oncolys BioPharma, Inc. No other potential conflicts of interest were disclosed.

Acknowledgments

We thank Daiju Ichimaru and Hitoshi Kawamura for their helpful discussions. We also thank Tomoko Sueishi for her excellent technical support.

Grant Support

Grants-in-Aid from the Ministry of Education, Science, and Culture, Japan (T. Fujiwara) and the Ministry of Health, Labour and Welfare, Japan (T. Fujiwara).

The costs of publication of this article were defrayed in part by the payment of page charges. This article must therefore be hereby marked *advertisement* in accordance with 18 U.S.C. Section 1734 solely to indicate this fact.

Received 06/19/2009; revised 03/26/2010; accepted 04/01/2010; published OnlineFirst 05/25/2010.

References

1. Grem JL. Biochemical modulation of 5-FU in systemic treatment of advanced colorectal cancer. Oncology (Williston Park) 2001;15:13–9.
2. Kumar S, Gao L, Yeagy B, Reid T. Virus combinations and chemotherapy for the treatment of human cancers. Curr Opin Mol Ther 2008;10:371–9.
3. Senzer N, Mani S, Rosemurgy A, et al. TNFerade biologic, an adenovector with a radiation-inducible promoter, carrying the human tumor necrosis factor α gene: a phase I study in patients with solid tumors. J Clin Oncol 2004;22:592–601.
4. Hollstein M, Sidransky D, Vogelstein B, Harris CC. p53 mutations in human cancers. Science 1991;253:49–53.
5. Levine AJ, Perry ME, Chang A, et al. The 1993 Walter Hubert lecture: the role of the p53 tumour-suppressor gene in tumorigenesis. Br J Cancer 1994;69:409–16.
6. Swisher SG, Roth JA, Nemunaitis J, et al. Adenovirus-mediated p53 gene transfer in advanced non-small-cell lung cancer. J Natl Cancer Inst 1999;91:763–71.
7. Nemunaitis J, Swisher SG, Timmons T, et al. Adenovirus-mediated p53 gene transfer in sequence with cisplatin to tumors of patients with non-small-cell lung cancer. J Clin Oncol 2000;18:609–22.
8. Swisher SG, Roth JA, Komaki R, et al. Induction of p53-regulated genes and tumor regression in lung cancer patients after intratumoral delivery of adenoviral p53 (INGN 201) and radiation therapy. Clin Cancer Res 2003;9:93–101.
9. Fujiwara T, Tanaka N, Kanazawa S, et al. Multicenter phase I study of repeated intratumoral delivery of adenoviral p53 in patients with advanced non-small-cell lung cancer. J Clin Oncol 2006;24:1689–99.
10. Bischoff JR, Kirn DH, Williams A, et al. An adenovirus mutant that replicates selectively in p53-deficient human tumor cells. Science 1996;274:373–6.
11. Rodriguez R, Schuur ER, Lim HY, Henderson GA, Simons JW, Henderson DR. Prostate attenuated replication competent adenovirus (ARCA) CN706: a selective cytotoxic for prostate-specific antigen-positive prostate cancer cells. Cancer Res 1997;57:2559–63.
12. Kirn D, Martuza RL, Zwiebel J. Replication-selective virotherapy for cancer: biological principles, risk management and future directions. Nat Med 2001;7:781–7.
13. Kawashima T, Kagawa S, Kobayashi N, et al. Telomerase-specific replication-selective virotherapy for human cancer. Clin Cancer Res 2004;10:285–92.
14. Umeoka T, Kawashima T, Kagawa S, et al. Visualization of intrathoracically disseminated solid tumors in mice with optical imaging by telomerase-specific amplification of a transferred green fluorescent protein gene. Cancer Res 2004;64:6259–65.
15. Taki M, Kagawa S, Nishizaki M, et al. Enhanced oncolysis by a tropism-modified telomerase-specific replication-selective adenoviral agent OBP-405 ('Telomelysin-RGD'). Oncogene 2005;24:3130–40.
16. Fujiwara T, Kagawa S, Kishimoto H, et al. Enhanced antitumor efficacy of telomerase-selective oncolytic adenoviral agent OBP-401 with docetaxel: preclinical evaluation of chemovirotherapy. Int J Cancer 2006;119:432–40.
17. Kishimoto H, Kojima T, Watanabe Y, et al. *In vivo* imaging of lymph node metastasis with telomerase-specific replication-selective adenovirus. Nat Med 2006;12:1213–9.
18. Blackburn EH. Structure and function of telomeres. Nature 1991;350:569–73.
19. Kim NW, Piatyszek MA, Prowse KR, et al. Specific association of

human telomerase activity with immortal cells and cancer. Science 1994;266:2011–5.
20. Shay JW, Wright WE. Telomerase activity in human cancer. Curr Opin Oncol 1996;8:66–71.
21. Nakayama J, Tahara H, Tahara E, et al. Telomerase activation by hTRT in human normal fibroblasts and hepatocellular carcinomas. Nat Genet 1998;18:65–8.
22. Fujiwara T, Tanaka N, Numunaitis JJ, et al. Phase I trial of intratumoral administration of OBP-301, a novel telomerase-specific oncolytic virus, in patients with advanced solid cancer: evaluation of biodistribution and immune response. J Clin Oncol 2008;26:3572.
23. Ohtani S, Kagawa S, Tango Y, et al. Quantitative analysis of p53-targeted gene expression and visualization of p53 transcriptional activity following intratumoral administration of adenoviral p53 *in vivo*. Mol Cancer Ther 2004;3:93–100.
24. Roth JA. Adenovirus p53 gene therapy. Expert Opin Biol Ther 2006; 6:55–61.
25. Kirn D. Oncolytic virotherapy for cancer with the adenovirus dl1520 (Onyx-015): results of phase I and II trials. Expert Opin Biol Ther 2001;1:525–38.
26. Hall AR, Dix BR, O'Carroll SJ, Braithwaite AW. p53-dependent cell death/apoptosis is required for a productive adenovirus infection. Nat Med 1998;4:1068–72.
27. Lee CT, Lee YJ, Kwon SY, et al. *In vivo* imaging of adenovirus transduction and enhanced therapeutic efficacy of combination therapy with conditionally replicating adenovirus and adenovirus-p27. Cancer Res 2006;66:372–7.
28. Li X, Raikwar SP, Liu YH, et al. Combination therapy of androgen-independent prostate cancer using a prostate restricted replicative adenovirus and a replication-defective adenovirus encoding human endostatin-angiostatin fusion gene. Mol Cancer Ther 2006;5:676–84.
29. Nemunaitis J, Tong AW, Nemunaitis M, et al. A phase I study of telomerase-specific replication competent oncolytic adenovirus (telomelysin) for various solid tumors. Mol Ther 2010;18: 429–34.
30. Chattopadhyay D, Ghosh MK, Mal A, Harter ML. Inactivation of p21 by E1A leads to the induction of apoptosis in DNA-damaged cells. J Virol 2001;75:9844–56.
31. Haviv YS, Takayama K, Glasgow JN, et al. A model system for the design of armed replicating adenoviruses using p53 as a candidate transgene. Mol Cancer Ther 2002;1:321–8.
32. Nanda D, Vogels R, Havenga M, Avezaat CJ, Bout A, Smitt PS. Treatment of malignant gliomas with a replicating adenoviral vector expressing herpes simplex virus-thymidine kinase. Cancer Res 2001; 61:8743–50.
33. Hioki M, Kagawa S, Fujiwara T, et al. Combination of oncolytic adenovirotherapy and Bax gene therapy in human cancer xenografted models. Potential merits and hurdles for combination therapy. Int J Cancer 2008;122:2628–33.

Telomerase-Dependent Oncolytic Adenovirus Sensitizes Human Cancer Cells to Ionizing Radiation via Inhibition of DNA Repair Machinery

Shinji Kuroda[1], Toshiya Fujiwara[1], Yasuhiro Shirakawa[1], Yasumoto Yamasaki[1], Shuya Yano[1], Futoshi Uno[1], Hiroshi Tazawa[2], Yuuri Hashimoto[1], Yuichi Watanabe[1,3], Kazuhiro Noma[1], Yasuo Urata[3], Shunsuke Kagawa[1], and Toshiyoshi Fujiwara[1,2]

Abstract

The inability to repair DNA double-strand breaks (DSB) leads to radiosensitization, such that ionizing radiation combined with molecular inhibition of cellular DSB processing may greatly affect treatment of human cancer. As a variety of viral products interact with the DNA repair machinery, oncolytic virotherapy may improve the therapeutic window of conventional radiotherapy. Here, we describe the mechanistic basis for synergy of irradiation and OBP-301 (Telomelysin), an attenuated type-5 adenovirus with oncolytic potency that contains the human telomerase reverse transcriptase promoter to regulate viral replication. OBP-301 infection led to E1B55kDa viral protein expression that degraded the complex formed by Mre11, Rad50, and NBS1, which senses DSBs. Subsequently, the phosphorylation of cellular ataxia-telangiectasia mutated protein was inhibited, disrupting the signaling pathway controlling DNA repair. Thus, tumor cells infected with OBP-301 could be rendered sensitive to ionizing radiation. Moreover, by using noninvasive whole-body imaging, we showed that intratumoral injection of OBP-301 followed by regional irradiation induces a substantial antitumor effect, resulting from tumor cell–specific radiosensitization, in an orthotopic human esophageal cancer xenograft model. These results illustrate the potential of combining oncolytic virotherapy and ionizing radiation as a promising strategy in the management of human cancer. *Cancer Res; 70(22); 9339–48. ©2010 AACR.*

Introduction

Current treatment strategies for advanced cancer include surgical resection, radiation, and cytotoxic chemotherapy. Preoperative or postoperative chemoradiation may improve local control and the survival of advanced cancer patients by minimizing the risk of dissemination during the surgical procedure, increasing the complete resection rate, and eradicating microscopic residual tumor cells that are not surgically removed. The lack of restricted selectivity for tumor cells is the primary limitation of radiotherapy, despite improved technologies such as stereotactic and hyperfractionated radiotherapy. Although radiotherapy is generally considered to be less invasive, the maximum doses and treatment fields are limited to avoid the influence on the surrounding normal tissues. Therefore, to improve the therapeutic index of radiotherapy while maintaining a tolerance of normal tissue toxicity, there is a need for agents that effectively lower the threshold for radiation-induced tumor cell death; the safety and efficacy of some candidates are already being explored in clinical trials (1–3).

Ionizing radiation primarily targets DNA molecules and induces double-strand breaks (DSB; ref. 4). Radiosensitization can result from a therapeutic increase in DNA DSBs or inhibition of their repair. Ataxia-telangiectasia mutated (ATM) protein is an important signal transducer of the DNA damage response, which contains DNA repair and cell cycle checkpoints, and activation of ATM by autophosphorylation occurs in response to exposed DNA DSBs (5). Cells mutated in the ATM gene have defects in cell cycle checkpoints and DNA repair and are hypersensitive to DSBs (6, 7); thus, agents that inhibit the ATM pathway can be useful radiosensitizers (8). The Mre11, Rad50, and NBS1 (MRN) complex is quickly stimulated by DSBs and directly activates ATM (9, 10). Defects in the MRN complex lead to genomic instability, telomere shortening, and hypersensitivity to DNA damage (11).

We reported previously that telomerase-specific, replication-selective adenovirus (Telomelysin, OBP-301), in which the human telomerase reverse transcriptase (hTERT) promoter element drives the expression of *E1* genes, induced selective

Authors' Affiliations: [1]Department of Gastroenterological Surgery, Okayama University Graduate School of Medicine, Dentistry and Pharmaceutical Sciences; [2]Center for Gene and Cell Therapy, Okayama University Hospital, Okayama, Japan; and [3]Oncolys BioPharma, Inc., Tokyo, Japan

Note: Supplementary data for this article are available at Cancer Research Online (http://cancerres.aacrjournals.org/).

Corresponding Author: Toshiyoshi Fujiwara, Department of Gastroenterological Surgery, Okayama University Graduate School of Medicine, Dentistry and Pharmaceutical Sciences, 2-5-1 Shikata-cho, Kita-ku, Okayama 700-8558, Japan. Phone: 81-86-235-7257; Fax: 81-86-221-8775; E-mail: toshi_f@md.okayama-u.ac.jp.

doi: 10.1158/0008-5472.CAN-10-2333

©2010 American Association for Cancer Research.

E1 expression, and efficiently killed human cancer cells but not normal human somatic cells (12–15). Adenoviral E1B55kDa protein, a gene product in the adenoviral early region, inhibits the functions of p53 and the MRN complex by cooperating with adenoviral E4orf6 protein, leading to the proteolytic degradation of these proteins (10, 16–18). In the present study, we showed the synergistic efficacy of combined treatment with ionizing radiation and OBP-301 against human cancer cells, and we clarified the E1B55kDa-mediated mechanism used by OBP-301 to inhibit DNA repair.

Materials and Methods

Cell lines and cell cultures

The human non–small-cell lung cancer cell line A549 was propagated in DMEM containing Nutrient Mixture (Ham's F-12) and supplemented with 10% FCS. The human esophageal squamous cell carcinoma cell line TE8 was cultured in RPMI 1640 supplemented with 10% FCS. The human esophageal adenocarcinoma cell line SEG1 was cultured in DMEM supplemented with 10% FCS. TE8 cells transfected with the firefly luciferase plasmid vector (TE8-Luc) were maintained in medium containing 0.2 mg/mL Geneticin (G418).

Adenovirus

The recombinant, replication-selective, tumor-specific adenovirus vector OBP-301 (Telomelysin), in which the hTERT promoter element drives the expression of *E1A* and *E1B* genes linked with an internal ribosome entry site, was previously characterized (12–15). The wild-type adenovirus type 5 (Ad-wt) and the E1B55kDa-defective adenovirus mutant dl1520 (Onyx-015) were also used (19).

Cell viability assay

A549, TE8, and SEG1 cells were infected with OBP-301 at the indicated multiplicities of infection (MOI) and then irradiated at the indicated dosages by using an MBR-1520R device (Hitachi Medical Co.). Cell viability was determined 5 days after irradiation with a Cell Proliferation Kit II (Roche Molecular Biochemicals), according to the manufacturer's protocol. Synergy between radiation and OBP-301 was analyzed with the CalcuSyn software (BioSoft), and the computation of the combination index was based on the methods of Chou and Talalay (20).

Flow cytometry

Cells were incubated for 20 minutes on ice in Cytofix/Cytoperm solution (BD Biosciences) and labeled with phycoerythrin (PE)-conjugated rabbit monoclonal active caspase-3 antibody (BD Biosciences) for 30 minutes and analyzed by FACSArray (BD Biosciences).

Immunofluorescence staining

Cells seeded on tissue culture chamber slides were treated and then fixed with cold methanol for 30 minutes on ice. The slides were subsequently incubated with primary antibody against pATM (Rockland), Mre11, Rad50 (GeneTex), NBS1 (Novus), and E1B55kDa (kindly provided by Dr. Arnold Levine, The Institute for Advanced Study, Princeton, NJ) for 1 hour on ice. After washing twice with PBS, slides were incubated with the secondary antibody, FITC-conjugated rabbit anti-mouse IgG (Zymed Laboratories), FITC-conjugated goat anti-rabbit IgG (Vector Laboratories), or Alexa 568–conjugated goat anti-mouse IgG (Molecular Probes), for 1 hour on ice. The slides were further stained with 4′,6-diamidino-2-phenylindole, mounted by using Fluorescent Mounting Medium (Dako Cytomation), and then analyzed with an LSM510 confocal laser microscope (Zeiss).

Western blot analysis

The primary antibodies against pATM (Cell Signaling), ATM (Novus), Mre11, Rad50, NBS1, E1B55kDa (kindly provided by Dr. Levine), γH2AX (Upstate), poly(ADP-ribose) polymerase (PARP; Cell Signaling), β-actin (Sigma), and peroxidase-linked secondary antibodies (Amersham) were used. Proteins were electrophoretically transferred to Hybond-polyvinylidene difluoride transfer membranes (GE Healthcare Life Science) and incubated with primary antibody, followed by peroxidase-linked secondary antibody. The Amersham ECL chemiluminescence system (GE Healthcare Life Science) was used to detect the peroxidase activity of the bound antibody.

In vivo subcutaneous human tumor model

A549, TE8, and SEG1 cells (2×10^6 per mouse) were injected s.c. into the flanks of 5- to 6-week-old female BALB/c *nu/nu* mice. When tumors reached ~3 to 5 mm in diameter, the mice were irradiated at a dosage of 3 Gy/tumor every 2 days (for A549) or 2 Gy/tumor every week (for TE8 and SEG1) for three cycles starting at day 0. When irradiated, mice were placed prone in custom-made holders that contain lead collimators to shield the upper half of the mice. Immediately after radiation, OBP-301 at a dose of 1×10^8 plaque-forming units (PFU)/tumor or PBS was injected into the tumor. In experiments with larger tumors, subcutaneous TE8 tumors with a diameter of 8 to 10 mm were treated with radiation at 2 Gy/tumor and intratumoral injection of OBP-301 at 1×10^8 PFU/tumor three times per week (every 2 days) for three cycles (nine times in total). The perpendicular diameter of each tumor was measured every 3 to 4 days, and tumor volume was calculated with the following formula: tumorvolume (mm^3) = $a \times b^2 \times 0.5$, where a is the longest diameter, b is the shortest diameter, and 0.5 is a constant to calculate the volume of an ellipsoid. The experimental protocol was approved by the Ethics Review Committee for Animal Experimentation of Okayama University.

Orthotopic human esophageal cancer model

TE8-Luc cells (2×10^6 per mouse) suspended in Matrigel were inoculated into the abdominal esophagus of 6-week-old female BALB/c *nu/nu* mice during laparotomy. Three weeks later, mice were irradiated with 2 Gy/tumor in holders that contain lead collimators to shield the head, neck, and chest of the mice. Immediately after radiation, mice were intratumorally injected with OBP-301 at 1×10^8 PFU/tumor during laparotomy, every 2 days for three cycles. To monitor tumor progression, the substrate luciferin was injected i.p. at a dose

of 150 mg/kg body weight. Images were collected in the supine position every few minutes from 10 to 30 minutes after luciferin injection with the IVIS Imaging System (Xenogen), and photons emitted from the abdominal esophagus region were quantified by using Living Image Software (Xenogen).

Statistical analysis

All data were expressed as mean ± SD. Differences between groups were examined for statistical significance with the Student's t test. P values <0.05 were considered statistically significant.

Results

Radiosensitizing effect of OBP-301 *in vitro*

To examine the potential interaction between OBP-301 and ionizing radiation *in vitro*, we first evaluated their combined effect in human lung (A549) and esophageal (TE8 and SEG1) cancer cell lines. The cells received a single dose of ionizing irradiation 24 hours after either mock or OBP-301 infection, and the cell viability was assessed by 2,3-bis[2-methoxy-4-nitro-*S*-sulfophenynl]*H*-tetrazolium-5-carboxanilide inner salt (XTT) assay 5 days after irradiation. The addition of OBP-301 increased the cytotoxicity of ionizing radiation in a dose-dependent manner. The combination index showed potent, statistically significant synergy between OBP-301 and radiation in all three cell lines (Fig. 1A). In contrast, synergy was not observed in normal human lung fibroblasts (NHLF) because the viral replication of OBP-301 was attenuated in telomerase-negative normal cells (Supplementary Fig. S2A, B).

We measured the amount of apoptosis in A549 and TE8 cells that were irradiated after OBP-301 infection. The cells were infected with OBP-301 at a MOI of 1.0, irradiated with a dose of 10 Gy 24 hours after infection, and analyzed for apoptosis. OBP-301 caused a significant increase in active caspase-3–positive cells in response to ionizing irradiation (Fig. 1B). Western blot analysis showed that ionizing radiation promoted the cleavage of PARP, a caspase-3 substrate and a biochemical marker of apoptosis, with prior OBP-301 infection (Fig. 1C). Moreover, OBP-301 infection before irradiation significantly increased the number of A549 cells with apoptotic nuclear morphology (Fig. 1D and E). Thus, OBP-301 combined with ionizing radiation synergistically increased the amount of apoptosis.

Degradation of the MRN complex by adenoviral E1B55kDa protein

To elucidate the molecular mechanism responsible for the synergy between OBP-301 and ionizing radiation, we examined the physical interaction between viral proteins and the MRN complex, which drives the DNA repair pathway as a sensor of DNA DSBs, through a series of confocal microscopy experiments. Immunofluorescence staining of A549 cells infected with OBP-301 at an MOI of 10 showed colocalization of the signals representing Mre11, NBS1, and Rad50, suggesting that these proteins exist as a complex. Moreover, there was marked overlap in the nuclear signals corresponding to adenoviral E1B55kDa and NBS1, indicating a direct interaction between the E1B55kDa protein and the MRN complex (Fig. 2A). Western blot analysis showed that the levels of Mre11, NBS1, and Rad50 protein gradually decreased after OBP-301 infection at an MOI of 10, as the E1B55kDa expression increased (Fig. 2B). The expression of the MRN complex remained unchanged in NHLF because E1B55kDa expression was absent after OBP-301 infection (Supplementary Fig. S2C).

To confirm the effect of adenoviral E1B55kDa on the MRN degradation, we compared the subcellular localization and degradation of Mre11 protein after infection with wild-type adenovirus (Ad-wt), an adenovirus mutant that lacked E1B55kDa (dl1520, Onyx-015), or OBP-301 in A549 cells. The Mre11 protein accumulated in the nucleus in a scattered pattern within 24 hours after OBP-301 or Ad-wt infection and then relocated to the perinuclear area and was degraded; however, the scattered nuclear signals of Mre11 remained largely undegraded 72 hours after dl1520 infection (Fig. 2C). We measured the proportions of the cells with each staining pattern (scattered, perinuclear, or degraded) to compare the subcellular dynamics of the Mre11 protein. OBP-301 and Ad-wt infection caused a rapid decrease in Mre11-positive cells compared with dl1520 infection (Fig. 2D and E), suggesting that the E1B55kDa protein is essential for the degradation of the MRN complex.

Inhibition of radiation-induced DNA damage responses by OBP-301

The MRN complex functions as a DSB sensor that activates the ATM-dependent signaling pathway, which coordinates cell cycle arrest with DNA repair. To further investigate the relationship between E1B55kDa and ATM activation, we examined the effect of OBP-301 infection on the radiation-induced phosphorylation of ATM (pATM) in A549 cells. Immunofluorescence analysis revealed spot signals of pATM throughout the nuclei 30 minutes after ionizing radiation; however, OBP-301 or Ad-wt infection (10 MOI) 24 hours before irradiation blocked the formation of pATM foci (Fig. 3A). Pretreatment with OBP-301 significantly reduced the number of pATM-positive cells compared with pretreatment with dl1520 lacking E1B55kDa (Fig. 3B). Western blot analysis also showed that ionizing radiation induced the phosphorylation of ATM, whereas expression of E1B55kDa by OBP-301 infection led to the degradation of the MRN complex, which was accompanied by a greatly reduced level of pATM (Fig. 3C). Following dl1520 infection, ATM phosphorylation was seen in the absence of E1B55kDa expression and MRN degradation.

We also investigated whether OBP-301 infection could abrogate the DNA repair process by using γH2AX, which is a sensitive indicator of DSBs. Ionizing radiation induced γH2AX expression as early as 30 minutes after treatment in both mock- and OBP-301–infected A549 cells. The levels of γH2AX protein gradually decreased as the DNA DSBs were repaired in mock-infected cells, but remained elevated in cells infected with OBP-301 24 hours before irradiation (Fig. 3D). Densitometric quantification revealed that the relative density of γH2AX/β-actin at 3 hours after irradiation decreased by 64% without prior OBP-301 infection, but decreased by only

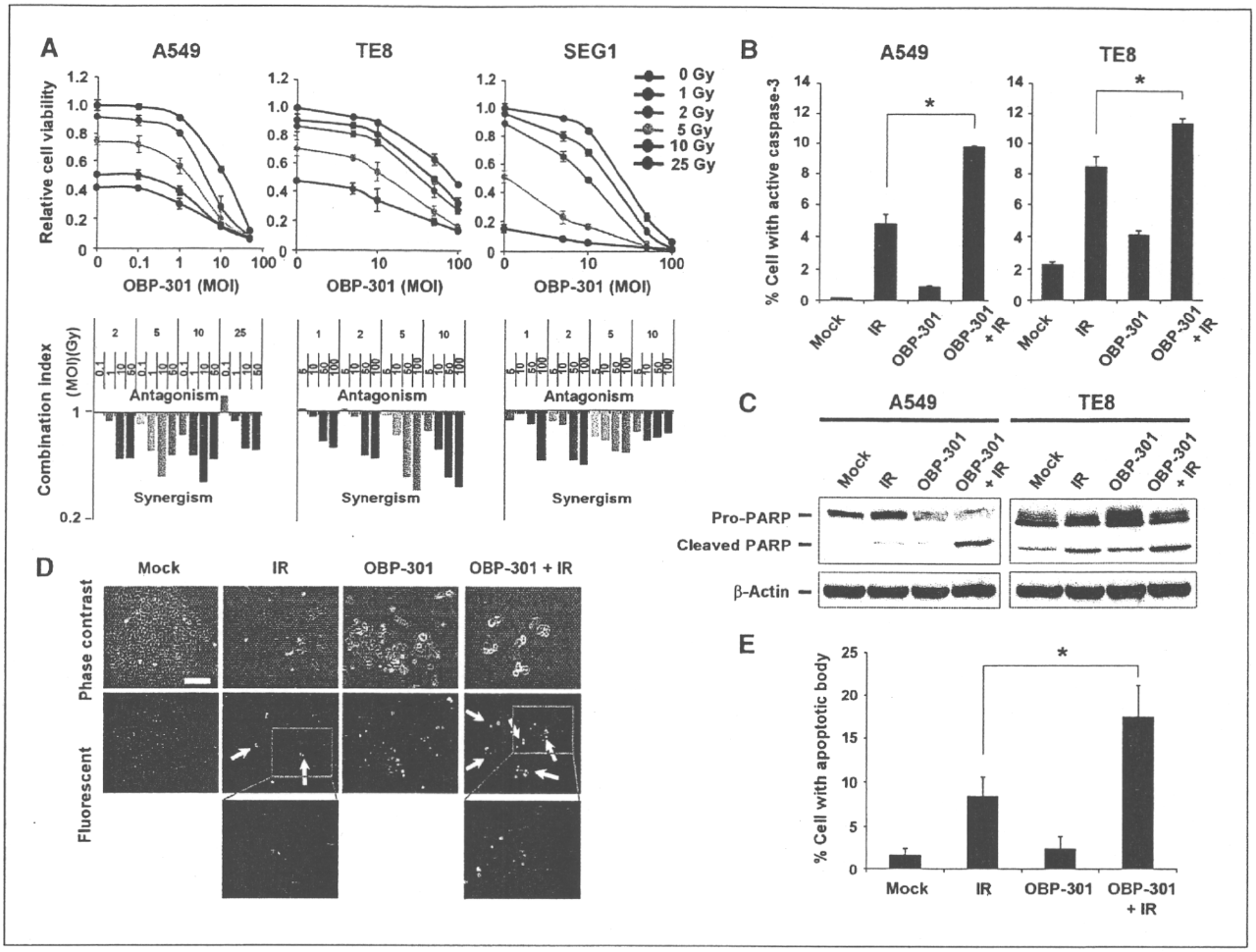

Figure 1. Radiosensitizing effect of OBP-301 on human cancer cells *in vitro*. A, cells were irradiated with the indicated doses 24 h after infection with OBP-301 at the indicated MOIs, and cell viability was assessed by XTT assay 5 d after irradiation. Top panels, percentages of viable cells relative to mock-treated cells. Error bars indicate 95% confidence intervals for triplicate data points. Bottom panels, the combination index was calculated with the CalcuSyn software. Synergy and antagonism were defined as interaction indices of <1 and >1, respectively. B to E, induction of apoptotic cell death by OBP-301 plus ionizing radiation. A549 and TE8 cells were infected with OBP-301 at an MOI of 1, irradiated with 10 Gy 24 h after infection, and then collected 5 d after irradiation. B, flow cytometric analysis for active caspase-3 expression. Cells were stained with PE-conjugated rabbit monoclonal active caspase-3 antibody and analyzed by FACS. *, $P < 0.01$. C, Western blot analysis for the cleavage of PARP. Blots were probed with anti-PARP antibody and visualized by using an ECL detection system. D, visualization of apoptotic nuclei. Treated A549 cells were stained with Hoechst 33342 and analyzed for DNA fragmentation by fluorescent microscopy. White arrows indicate cells with apoptotic bodies. The bottom panels are the magnified views of the boxed region in the middle panels. IR, ionizing radiation. E, the percentage of apoptotic cells was calculated by counting the number of cells with apoptotic bodies per 100 cells in six random fields in each group.

19% with OBP-301 infection compared with the levels at 30 minutes postirradiation (Fig. 3E). These results indicate that OBP-301 infection interrupts the cellular DNA repair mechanism induced by ionizing radiation.

Synergistic antitumor activity of OBP-301 plus radiation in human tumor xenografts

We next assessed the therapeutic efficacy of OBP-301 in combination with ionizing radiation against A549, TE8, and SEG1 cells *in vivo*. To determine the treatment schedule, we examined whether radiation could modify adenoviral infectivity and replication in human cancer cells. OBP-301 infection following ionizing radiation showed synergistic antitumor effects *in vitro* (Supplementary Fig. S3) due to an increased expression density of coxsackievirus and adenovirus receptor, which resulted in enhanced adenoviral uptake in human cancer cells (Supplementary Figs. S4 to S6). We also confirmed that ionizing radiation does not interfere with OBP-301 replication (Supplementary Fig. S7).

Based on these preliminary results, we chose a therapy regimen with three cycles of regional radiation followed immediately by intratumoral administration of OBP-301. Mice bearing A549, TE8, and SEG1 subcutaneous tumors that were 3 to 5 mm in diameter received 3 Gy (for A549) or 2 Gy (for TE8 and SEG1) local irradiation followed by the intratumoral injection of either 1×10^8 PFU of OBP-301 or PBS every 2 days (for A549) or 7 days (for TE8 and SEG1) for three cycles. Intratumoral administration of OBP-301 or radiation

alone resulted in significant tumor growth suppression compared with mock-treated tumors. The combination of OBP-301 plus radiation produced a more profound and significant inhibition of tumor growth compared with either modality alone in all three types of tumors, despite the difference in treatment schedules (Fig. 4A).

Histopathologic analysis of A549 tumors excised 10 days after the completion of three cycles of either regional radiation or OBP-301 infection revealed the degeneration of tissues and reduced tumor cell density compared with untreated tumors. However, treatment with OBP-301 injection plus radiation yielded massive tissue destruction and further reduction in tumor cell density. Moreover, the cytolytic changes induced by the combination therapy led to the development of hyalinized acellular stroma (Fig. 4B). Terminal deoxyribonucleotidyl transferase-mediated dUTP nick end labeling (TUNEL) staining showed that combining ionizing radiation with OBP-301 markedly increased the amount of apoptotic cells in A549 tumors excised 3 days after the completion of the treatment (Fig. 4C). OBP-301 plus irradiation apparently increased PARP cleavage in A549 tumors compared with ionizing radiation alone (Fig. 4D).

Eradication of established human tumor xenografts by OBP-301 plus radiation

To mimic the clinical characteristics of advanced cancer patients, we established TE8 xenografts with a 10-fold larger tumor burden. Mice bearing large TE8 subcutaneous tumors received nine cycles of 2 Gy irradiation followed by intratumoral injection of 1×10^8 PFU of OBP-301 three times per week for 3 weeks. Tumors treated with either OBP-301 or ionizing radiation alone exhibited a transient shrinkage,

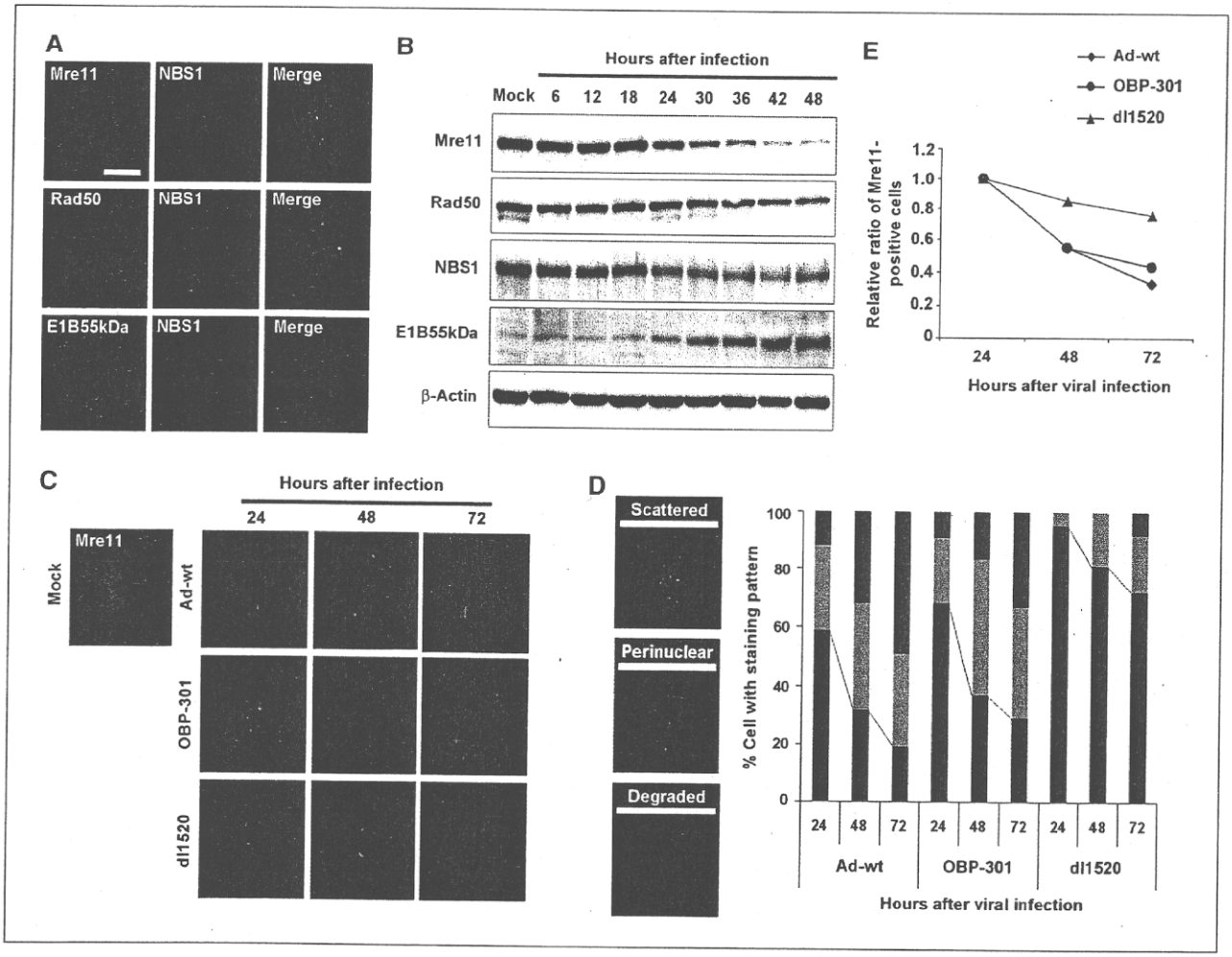

Figure 2. Degradation of the MRN complex by E1B55kDa protein. A, A549 cells were infected with OBP-301 at an MOI of 10 and then stained for NBS1 and either Mre11, Rad50, or E1B55kDa 24 h after infection. The localization of these proteins was visualized by confocal laser microscopy. Scale bar, 100 μm. B, A549 cells were infected with OBP-301 at an MOI of 10 and collected at the indicated time points after infection. Blots were probed with antibodies for Mre11, Rad50, NBS1, and E1B55kDa. C, A549 cells were infected with either Ad-wt, OBP-301, or dl1520 (Onyx-015) at an MOI of 10; stained for Mre11 at 24, 48, and 72 h after infection; and analyzed by confocal laser microscopy. D, the subcellular distribution of Mre11 protein was classified as scattered, perinuclear, and degraded. The proportions of each pattern were determined 24, 48, and 72 h after viral infection. E, quantification of Mre11-positive cells after OBP-301 infection. The relative ratios of cells with scattered staining are plotted against the amount of time since infection.

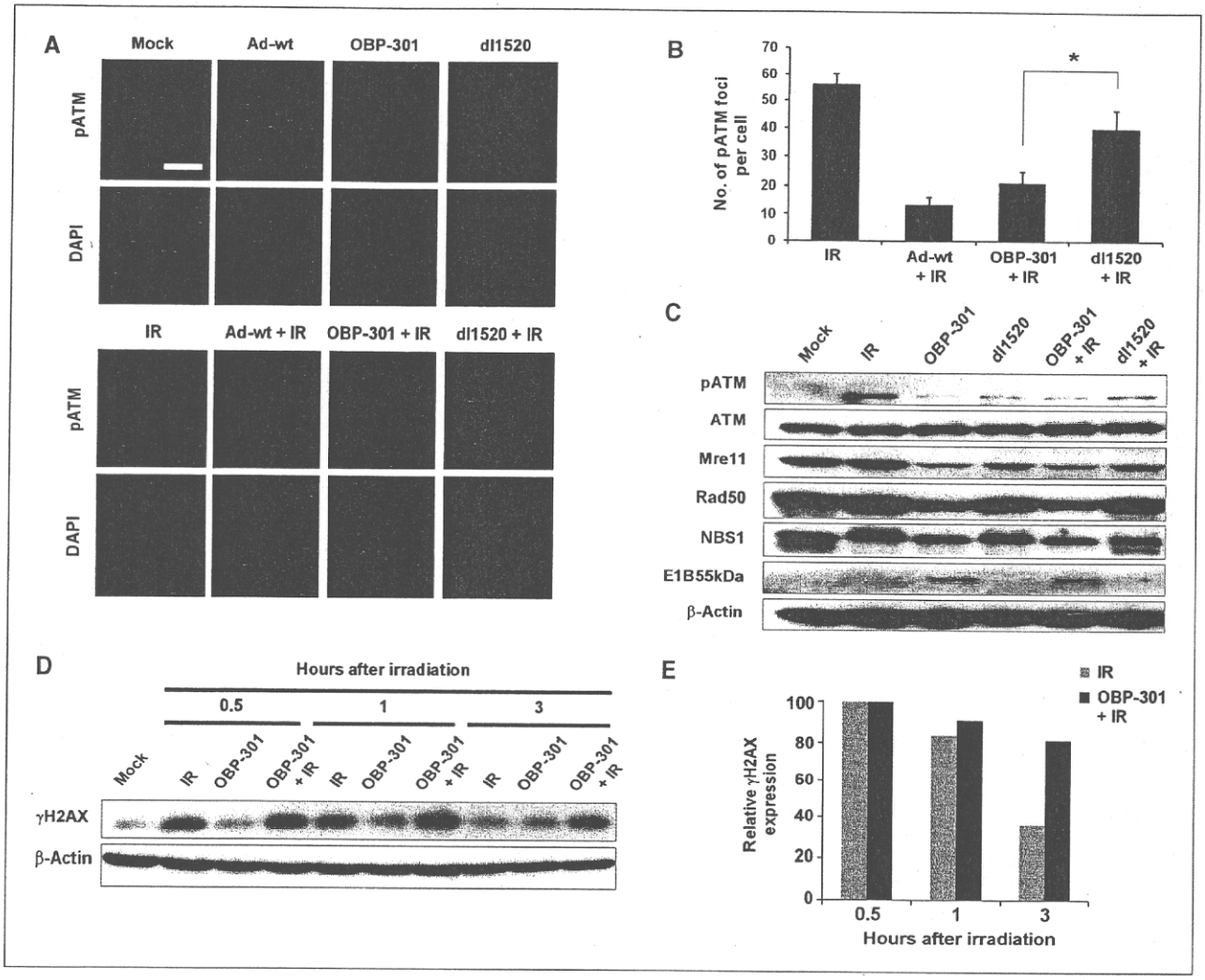

Figure 3. Inhibition of DNA repair by E1B55kDa protein through the blockade of radiation-induced ATM autophosphorylation. A, A549 cells were infected with either Ad-wt, OBP-301, or dl1520 at an MOI of 10 and then irradiated with 10 Gy at 24 h after infection. Nuclear phosphorylated ATM (pATM) foci were visualized 30 min after irradiation by immunofluorescent staining under a confocal laser microscope. Scale bar, 100 μm. B, quantification of pATM foci in treated A549 cells. The numbers of pATM foci per cell were counted in 10 different cells per group. *, $P < 0.01$. C, A549 cells were infected with OBP-301 or dl1520 and irradiated with 10 Gy at 24 h after infection. Cells were then subjected to Western blot analysis for pATM, ATM, Mre11, Rad11, NBS1, E1B55kDa, and β-actin 30 min after irradiation. D, γH2AX expression after irradiation in cells with or without OBP-301 infection. A549 cells were infected with OBP-301 at an MOI of 10 and then irradiated with 10 Gy at 24 h after infection. The cells were harvested at 0.5, 1, and 3 h after irradiation and subjected to Western blot analysis for γH2AX. Note the maintenance of γH2AX in the presence of OBP-301 infection. E, the levels of γH2AX expression were quantified by densitometric scanning with Image J software. The relative γH2AX expression is shown as a percentage of the γH2AX/β-actin value at 30 min after irradiation.

but invariably started to regrow 14 days after the beginning of treatment, whereas OBP-301 plus radiation completely eradicated the established larger TE8 tumors on day 28 in 9 of 10 mice (Fig. 5A).

Tumors treated with OBP-301 or radiation alone were consistently smaller than tumors of the control cohort of mice (Fig. 5B; Supplementary Fig. S8A). Massive ulceration was noted on the tumor surface after injection of OBP-301, whereas no tumor burden was detected when ionizing radiation was combined with OBP-301 injection. Moreover, histologic analysis revealed the apparent destruction of tumor tissues after OBP-301 injection or ionizing radiation. However, no residual tumor cells were observed in tumors treated with OBP-301 plus radiation; instead, massive cellular infiltrates were noted (Supplementary Fig. S8B). Mice with tumor eradication significantly recovered their body weight, although there was a gradual decrease in the body weight of the control group (Supplementary Fig. S9).

Evaluation of *in vivo* antitumor effects on orthotopic human esophageal cancer model

Finally, we assessed the therapeutic efficacy of intratumoral injection of OBP-301 and local irradiation in an orthotopic human esophageal cancer xenograft model by

using noninvasive whole-body imaging. When TE8 human esophageal cancer cells stably transfected with the luciferase gene (TE8-Luc) were s.c. implanted into nude mice, a correlation was observed between tumor growth (volume) and the luciferase emission level (luminescent intensity; Supplementary Fig. S10). Our preliminary experiments revealed that when TE8-Luc cells were inoculated into the wall of the abdominal esophagus of athymic *nu/nu* mice, esophageal tumors appeared within 3 weeks after tumor injection (Fig. 5C).

Mice bearing macroscopic esophageal tumors were treated with local irradiation at 2 Gy followed by intratumoral injection during laparotomy of 1×10^8 PFU of OBP-301 every 2 days for three cycles. The luminescent intensity of tumors treated with OBP-301 plus radiation was significantly lower than that of mock-treated, irradiated, or OBP-301–injected tumors (Fig. 5D and E). These results suggest that the biochemical interaction of OBP-301 with irradiation can be translated into a potential clinically applicable cancer treatment.

Discussion

A novel biological property of OBP-301 as a molecular radiosensitizer was verified, referring to a critical role of adenoviral E1B55kDa in inhibiting the DNA damage responses triggered by ionizing radiation. Radiation-induced cell death is dependent on DNA damage and, therefore, inhibition of

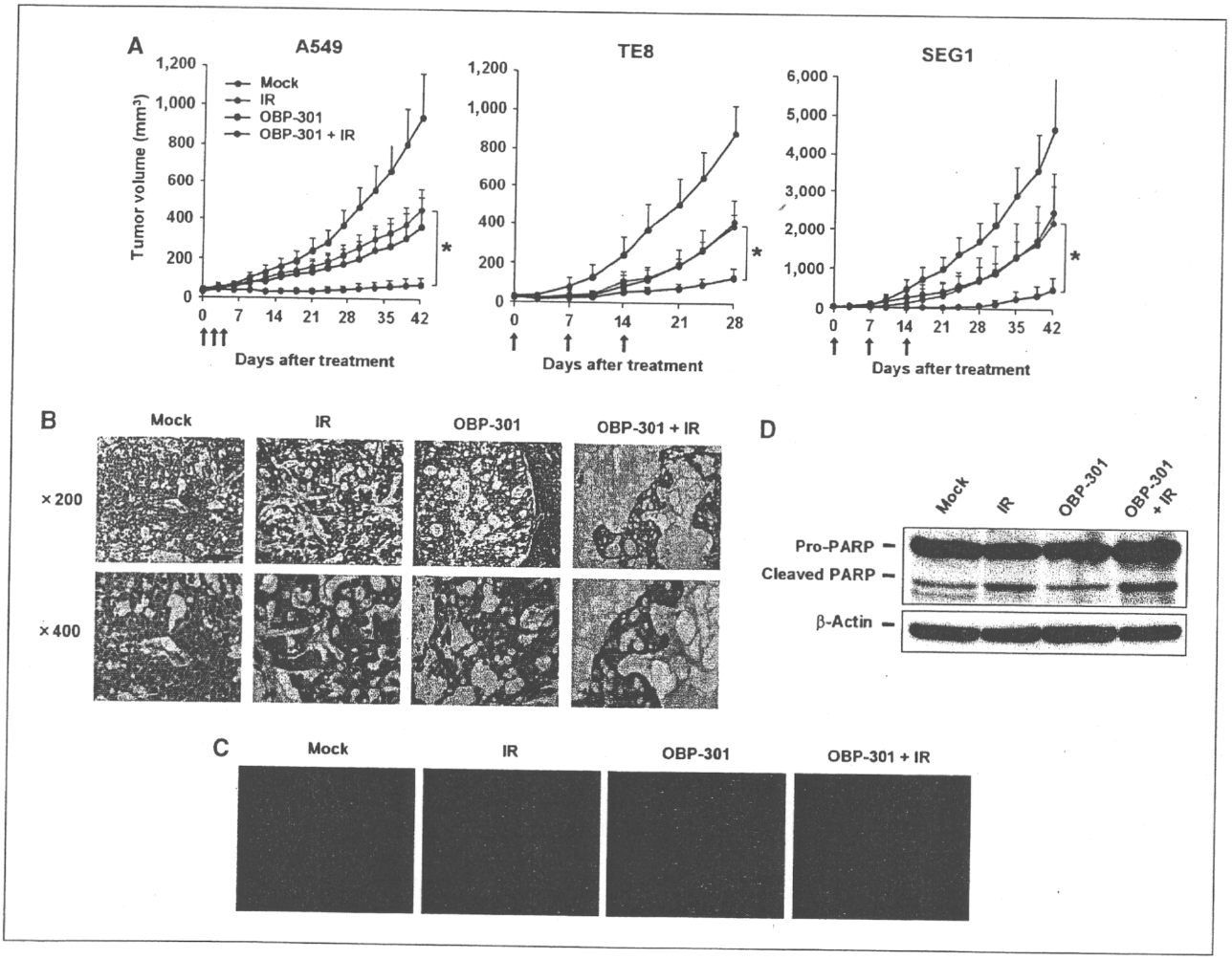

Figure 4. Antitumor effects of OBP-301 and ionizing radiation against s.c. established xenograft tumors. A, cells (2×10^6 per mouse) were injected s.c. into the right flanks of mice. When the tumors reached 3 to 5 mm in diameter, mice were exposed to 3 Gy (for A549) or 2 Gy (for TE8 and SEG1) of ionizing radiation and intratumorally administered OBP-301 (1×10^8 PFU/tumor) for three cycles every 2 d (for A549) or every week (for TE8 and SEG1). Six (for A549) or eight (for TE8 and SEG1) mice were used for each group. Tumor growth is expressed as the mean tumor volume ± SD. Arrows indicate each treatment. *, $P < 0.01$. B, mice bearing A549 xenografts were treated as described above. Tumor sections were obtained 10 d after the final administration of OBP-301. Paraffin sections of tumors were stained with hematoxylin and eosin. Scale bar, 100 μm. Magnification, ×200 (top), ×400 (bottom). C and D, *in vivo* induction of apoptotic cell death by OBP-301 and ionizing radiation. C, paraffin-embedded sections of A549 subcutaneous tumors excised 3 d after treatment as described above were subjected to TUNEL staining. D, Western blot analysis for PARP and β-actin was done with proteins extracted from A549 subcutaneous tumors 3 d after treatments.

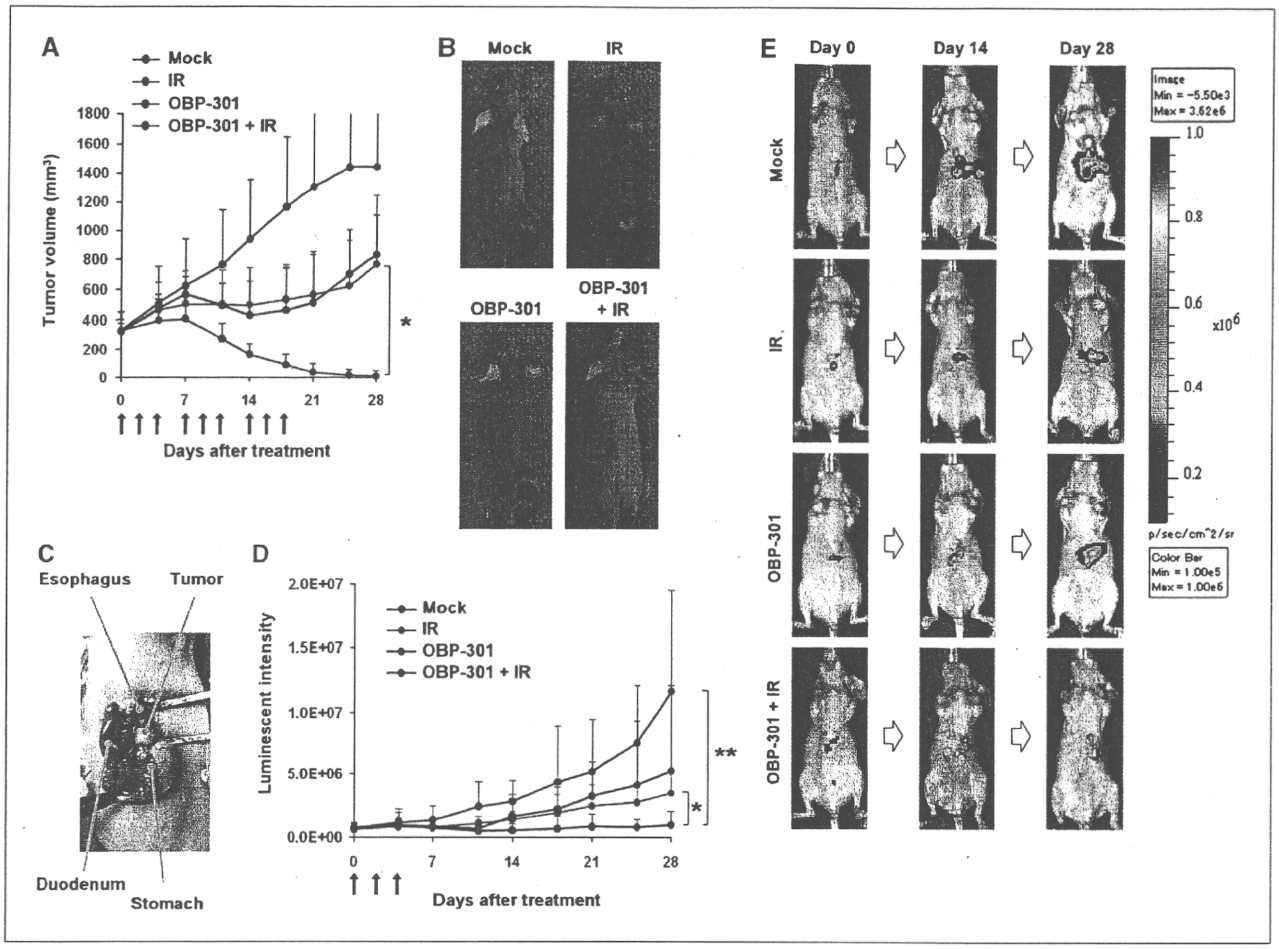

Figure 5. *In vivo* antitumor effects of OBP-301 and ionizing radiation against TE8 human esophageal cancer xenografts. A, larger subcutaneous TE8 tumors with a diameter of 8 to 10 mm were treated with OBP-301 followed by ionizing radiation three times per week (every 2 d) for three cycles (nine times in total). Ten mice were used for each group. Tumor growth is expressed as mean tumor volume ± SD. Arrows indicate each treatment. *, $P < 0.01$. B, macroscopic appearance of representative tumors 28 d after treatment. C, macroscopic appearance of orthotopic TE8-Luc esophageal tumor 3 wk after tumor cell inoculation (2×10^6 cells per mouse). D, mice bearing orthotopic TE8-Luc tumors were exposed to 2 Gy of ionizing radiation and intratumorally administered OBP-301 (1×10^8 PFU/tumor) for three cycles every 2 d. The luminescent intensity was measured by the IVIS imaging system 10 to 30 min after peritoneal administration of luciferin. Tumor growth is expressed by the luminescent intensity ± SD. Arrows indicate each treatment. *, $P < 0.01$; **, $P < 0.05$. E, representative images of mice treated with either ionizing radiation, OBP-301, or both on days 0, 14, and 28.

DNA repair can enhance the sensitivity of human tumor cells to ionizing radiation. The ATM activation by the MRN complex is essential for sensing and signaling from DNA DSBs and plays an important role in DNA repair and checkpoints, indicating that this pathway may be a good target for enhancing the antitumor effects of DNA-damaging agents. Indeed, ATM inhibitors, such as KU55933 and CGK733, and an MRN complex inhibitor, mirin, could sensitize cancer cells to therapeutic agents that cause DNA DSBs (21–23). Hsp90 interacts with the MRN complex, and an Hsp90 inhibitor enhances the sensitivity of tumor cells to radiation (24). Molecular disruption of MRN function by a dominant-negative mutant *Rad50* gene transfer sensitizes tumor cells to cisplatin (25). Although these approaches are effective in interrupting cellular DNA repair mechanisms, they lack tumor selectivity and may damage normal tissues when combined with DNA-damaging therapies. Our data show that OBP-301 could synergize with ionizing radiation only in tumor cells but not in normal cells due to its telomerase dependency, suggesting that the regional administration of OBP-301 enables targeted radiosensitization.

The adenovirus *E1B* gene encodes a 19-kDa polypeptide (*E1B19kDa*) and a 55-kDa protein (*E1B55kDa*). The E1B55kDa protein induces a cellular environment conducive for viral protein synthesis via a complex with the E4orf6 protein (26). This E1B55kDa/E4orf6 complex degrades the MRN complex, blocks the downstream ATM signaling, and leads to a defective G_2-M checkpoint in response to DSBs (10). Although the impact of E1B55kDa-mediated disruption of the MRN-ATM pathway on the DNA damage responses triggered by ionizing radiation has not yet been studied, we showed that OBP-301–mediated E1B55kDa expression induced the degradation of all components of the MRN

complex, which in turn prevented ATM autophosphorylation following ionizing radiation. OBP-301 expresses the *E1B* gene under the control of the hTERT promoter through an internal ribosome entry site sequence, whereas dl1520 (Onyx-015, CI-1042), which has been used in many clinical trials, was genetically modified by disruption of the coding sequence of the E1B55kDa protein (19). Therefore, ionizing radiation–induced ATM activation was blocked more efficiently by OBP-301 than by dl1520, which lacks E1B55kDa, although dl1520 slightly inhibited ATM phosphorylation, presumably due to E4orf6 protein expression (27).

One hallmark of DNA DSBs is the phosphorylation of H2AX at Ser139, a specialized histone H2A variant (referred to as γH2AX; ref. 28); the reduction in γH2AX levels in irradiated cells correlates with the repair of DSBs (29). OBP-301 infection apparently sustained the elevated levels of γH2AX longer in irradiated tumor cells, indicating that tumor cells infected with OBP-301 could be rendered sensitive to ionizing radiation. We previously found that the process of oncolysis is morphologically distinct from apoptosis and necrosis, although autophagy is partially involved in this effect (30). The observation that OBP-301 infection significantly enhanced the induction of apoptosis when combined with ionizing radiation suggests that the radiosensitizing activity of OBP-301 is independent of virus-mediated oncolysis. Indeed, dephosphorylation of H2AX is associated with efficient DNA repair, whereas a pronounced increase in H2AX phosphorylation correlates with apoptosis (31, 32). Moreover, synergistically enhanced apoptosis by OBP-310 and ionizing radiation is likely to be p53 independent because p53 was ubiquitinated and degraded by E1B55kDa and E4orf6 proteins (16, 18).

Our *in vitro* studies suggest that OBP-301 infection and ionizing radiation may mutually sensitize human tumor cells, potentially leading to an effective combination treatment. OBP-301 infection requires a period of replication to induce the cytopathic effect and to sensitize cells to radiation, whereas ionizing radiation immediately causes DNA DSBs. Therefore, in a true clinical setting, multiple cycles of the external-beam radiotherapy followed by intratumoral injection of OBP-301 may yield optimal results. We confirmed the synergistic antitumor effect of three cycles of treatment with OBP-301 plus regional radiation and the *in vivo* induction of apoptotic cell death on subcutaneous human tumor xenografts. The orthotopic implantation of tumor cells, however, restores the correct tumor-host interactions, which do not occur when tumors are implanted in ectopic subcutaneous sites (33). Thus, we also showed the significant synergy of combined treatments in an orthotopic mouse model of human esophageal cancer by using a noninvasive whole-body imaging system.

There are some possible advantages of combining virotherapy with radiotherapy *in vivo*. First, OBP-301 may inhibit the vascular supply by killing endothelial cells because endothelial cell proliferation is increased in irradiated tumors (34), presumably with high telomerase activity. Alternatively, local irradiation itself may attack the vascular endothelial cells in the tumor site, which in turn can block the escape of locally injected OBP-301 into the blood circulation. Indeed, ionizing radiation inhibits endothelial cell proliferation, tube formation, migration, and clonogenic survival (35). Furthermore, in an immunocompetent environment, as we previously reported (36), OBP-301 stimulates host immune cells to produce endogenous antiangiogenic factors such as interferon-γ. Second, virotherapy and radiotherapy may target tumor cells in different parts of tumors with distinct mechanisms. For example, tumor hypoxia has been considered a potential therapeutic problem because it renders tumor cells more resistant to ionizing radiation (37) and, therefore, some cells in certain parts of tumors may survive and proliferate under hypoxic conditions. In contrast, because hypoxia induces the transcriptional activity of hTERT gene promoter through hypoxia-inducible factor 1α (38), OBP-301 can be expected to replicate and efficiently kill tumor cells even under hypoxic conditions. Thus, hTERT-specific oncolytic virotherapy can be effective in eliminating tumor cells that survive after local radiotherapy.

Another advantage of this combination therapy is that the area where each treatment shows the therapeutic effect is overlapping. The treatment field of radiotherapy includes primary tumors and regional lymph nodes. We previously showed that intratumorally injected OBP-301 expressing the *GFP* gene is effectively transported into the lymphatic circulation; viral replication produced GFP fluorescence signals in the metastatic lymph nodes in orthotopic human colorectal and oral cancer xenograft models (39, 40). Therefore, we anticipate that intratumoral OBP-301 administration will radiosensitize both primary tumors and regional lymph nodes.

In summary, our data show the molecular basis of radiosensitization induced by telomerase-specific virotherapy, in which the adenoviral E1B55kDa protein inhibits the radiation-induced DNA repair machinery through the interruption of the MRN function. OBP-301 infection and ionizing radiation mutually modulate their respective biological effects and thereby potentiate each other, profoundly enhancing *in vivo* antitumor activity in an orthotopic mouse model.

Disclosure of Potential Conflicts of Interest

Y. Urata is an employee of Oncolys BioPharma, Inc., the manufacturer of OBP-301 (Telomelysin). The other authors disclosed no potential conflicts of interest.

Acknowledgments

We thank Dr. Frank McCormick (University of California at San Francisco Helen Diller Family Comprehensive Cancer Center) for supplying the E1B55kDa-defective adenovirus mutant dl1520 (Onyx-015), and Tomoko Sueishi and Mitsuko Yokota for their excellent technical support.

Grant Support

Ministry of Education, Culture, Sports, Science, and Technology of Japan (Toshiyoshi Fujiwara) and Ministry of Health, Labour, and Welfare of Japan (Toshiyoshi Fujiwara).

The costs of publication of this article were defrayed in part by the payment of page charges. This article must therefore be hereby marked *advertisement* in accordance with 18 U.S.C. Section 1734 solely to indicate this fact.

Received 06/29/2010; revised 09/13/2010; accepted 09/17/2010; published OnlineFirst 11/02/2010.